

## **Chapter III**

### **THE CONTENDAS-MIRANTE VOLCANO-SEDIMENTARY BELT**

**MOACYR M.MARINHO<sup>1</sup>; PIERRE SABATÉ<sup>2,3</sup> and JOHILDO S.F.BARBOSA<sup>3</sup>**

<sup>1</sup>CBPM - Companhia Baiana de Pesquisa Mineral, 4<sup>a</sup> Av., 460, CAB, 41206, Salvador, Bahia, Brazil

<sup>2</sup>ORSTOM, C. Postal 4741, Shopping Barra, 40149-900 Salvador, Bahia, Brazil

<sup>3</sup>Curso de Pós-Graduação em Geologia, PPPG - Programa de Pesquisa e Pós-Graduação em Geofísica, Instituto de Geociências, Universidade Federal da Bahia, Rua Caetano Moura, 123, Federação, 40210-350, Salvador, Bahia, Brazil

## INTRODUCTION

The Contendas-Mirante volcano-sedimentary belt (Fig. III.1) lies along an approximately 190 km long and 65 km wide North-South synform pinched between the granulitic eastern Jequié block and the medium-grade gneiss-migmatite-granite terrains of the western Gavião block (Marinho & Sabaté, 1982). It branches into smaller belts, to north and south, interfingering with the gneiss-migmatite-granite terrains. To northwest, the belt and its contacts with the Gavião block are covered by Middle and Upper Proterozoic platformal sediments.

The belt itself is made up of supracrustal formations, metamorphosed in the western part of the belt in the greenschist facies and progressively changing eastwards to amphibolite facies. The contact of the supracrustals with the catazonal lithotypes of the Jequié block is sharp and controlled by shearing and overthrusting (Sabaté & Gomes, 1984). Similarly, there is a sharp change from the epimetamorphic supracrustals to the medium-grade terrains of the Gavião block to the west, also with tectonic contacts.

The synformal belt can be subdivided into minor domical antiforms pinched between straight elongated synforms. It encloses the volcano-sedimentary sequence and several nuclei of gneiss-migmatite-granitoid associations which are related to the Gavião block. These nuclei outcrop in the domical structures and probably represent the basement of the belt formations.

The first attempt to subdivide the volcano-sedimentary sequence resulted in the identification of two main units and several subunits (Marinho et al., 1979, 1980). More recently, Marinho (1991) defined three lithostratigraphic units, separated by unconformities, for that sequence. The lower unit is essentially made up of volcanogenic rocks, while the middle and upper units are composed by clastic sediments.

The Contendas-Mirante sequence is intruded by mafic sills and several granitoid

plutons. The aligned younger plutonic rocks are typically peraluminous granites which postdate the orogenic evolution of the belt.

## GEOLOGIC SETTING OF THE AREA

### THE BASEMENT DOMES

The southern part of the Contendas-Mirante belt is composed of imbricated slices which juxtapose tectonic prisms of the supracrustal sequence with uplifted crustal segments related to the Gavião block basement and emplaced into the domical antiforms (Marinho & Sabaté, 1982; Sabaté & Gomes, 1984; Sabaté et al., 1988). These crustal segments also exhibit internal domical structures.

Three domes were recognized: (i) The Sete Voltas, (ii) the Boa Vista/Mata Verde and (iii) the Serra dos Meiras domes (Fig. III.2). The first two were intensively studied (Marinho et al., 1978, 1979, 1980; Cordani et al., 1985; Martin & Sabaté, 1990; Martin et al., 1991, 1992; Marinho, 1991).

### The Sete Voltas Dome

The Sete Voltas dome belongs to a huge N-S tectonic slice 60 km long and 10 km wide composed of gneisses, granitoids and migmatites. In the northern part of the slice the Sete Voltas meta-granitic batholith occurs.

This batholith is composed of banded or foliated gneisses and an irregularly deformed porphyritic granitoid which occupy the central part of the dome.

The oval shape and the sharp contact with the supracrustal host rock indicate an intrusive emplacement. However the strong ductile deformation parallel to the contacts and the presence of shear bands and faults on its boundaries, combined with the induction in the host rocks of shears with increasing strain nearby the contact show the mechanical character of the emplacement, interpreted as a forced non-magmatic intrusion (Sabaté & Gomes, 1984;

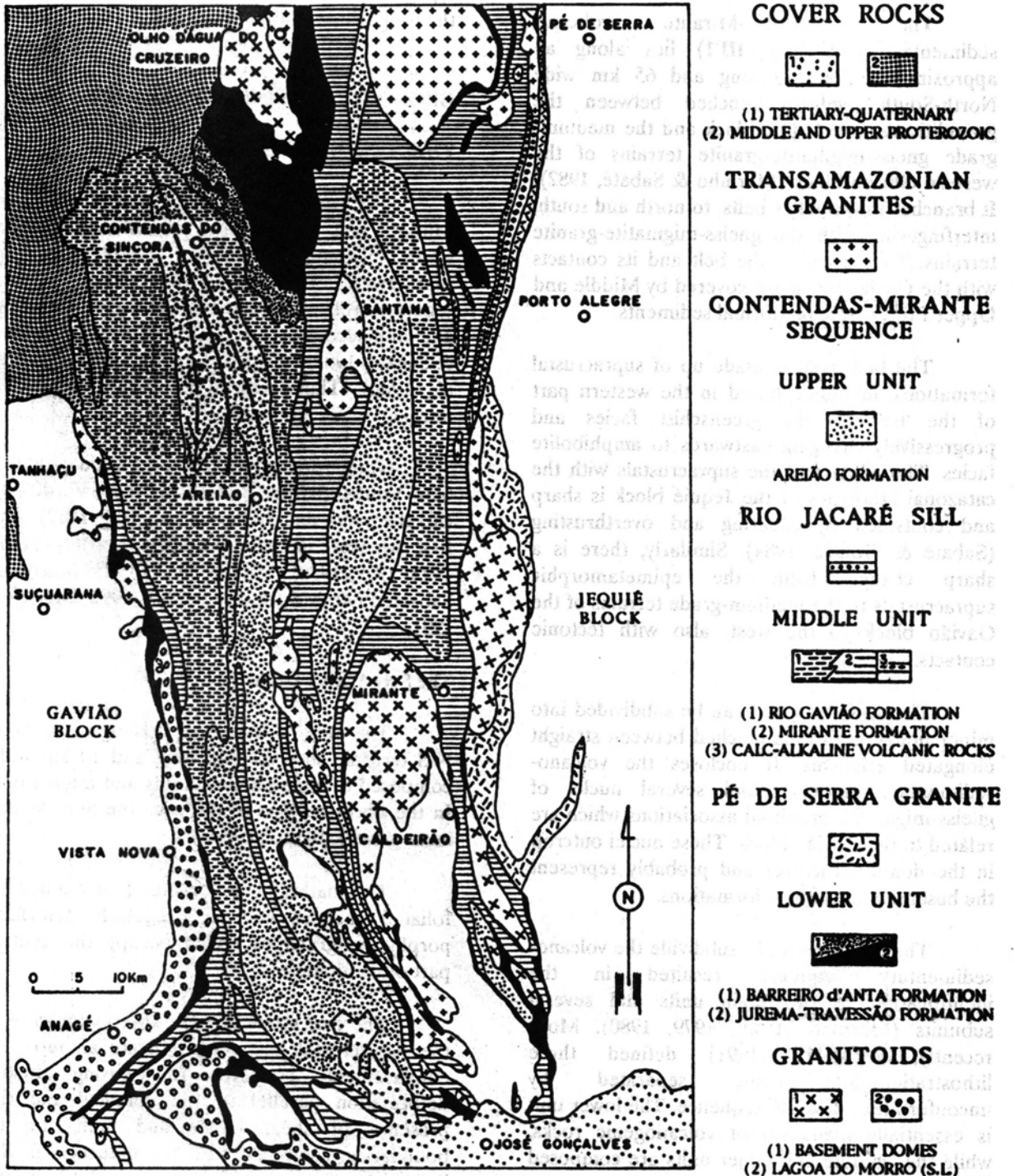


Figure III.1 - Stratigraphic sequence of the Contendas-Mirante volcano-sedimentary belt (after Marinho, 1991).

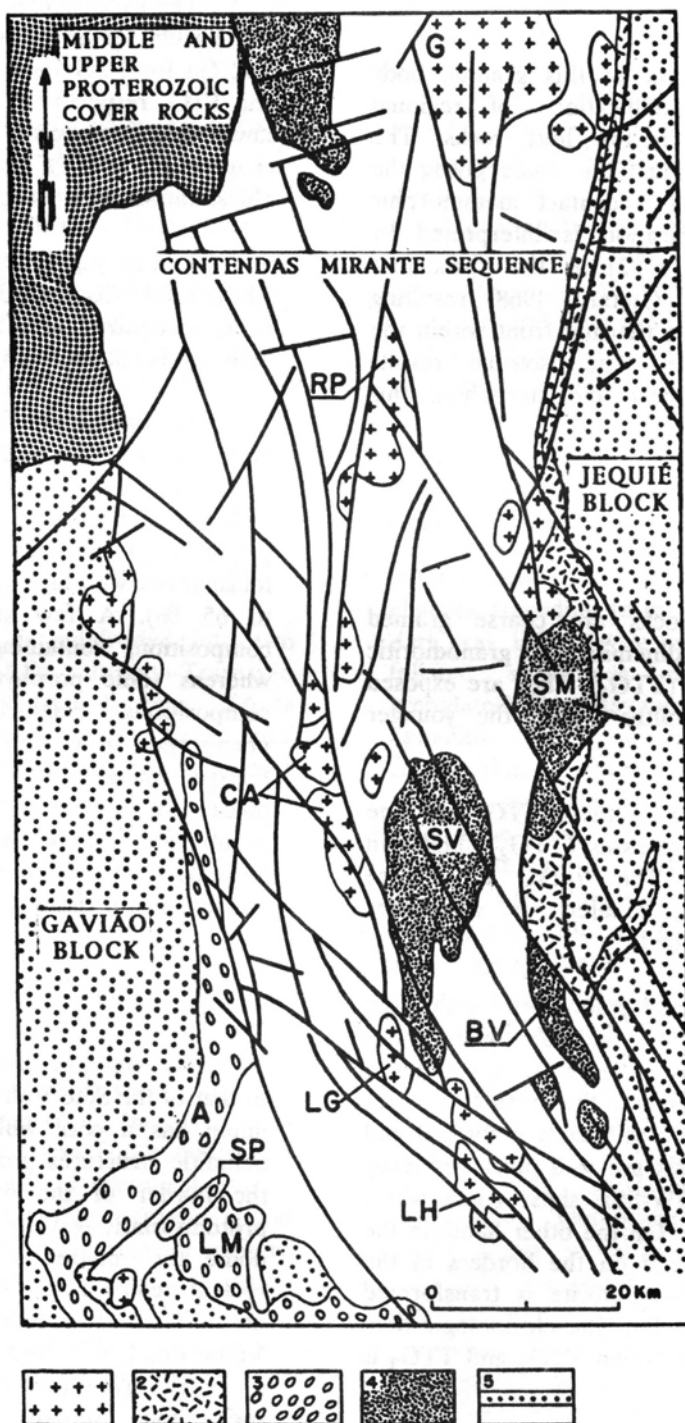


Figure III.2 - Geologic distribution of granitoid bodies and the Rio Jacaré mafic-ultramafic sill in the Contendas-Mirante volcano-sedimentary belt (after Marinho & Sabaté, 1982): 1. Transamazonian granites (G - Gameleira, RP - Riacho das Pedras, CA - Caetano/Aliaça, LG - Lagoa Grande, LH - Lagoinha); 2. Pé de Serra granite; 3. (A - Anagé/Pau de colher, LM - Lagoa do Morro, SP - Serra dos Pombos); 4. Basement Domes (SV - Sete Voltas, BV - Boa Vista/Mata Verde, SM - Serra dos Meiras); 5. Rio Jacaré Sill (after Marinho & Sabaté, 1982).

Sabaté et al., 1988).

The emplacement of this granitic body induced strong modifications of regional metamorphic zones in the host rocks. The isogrades tightly surround the dome giving the cartographic image of a contact metamorphic aureole. This configuration is interpreted by Marinho & Sabaté (1982) as the "basement effect" (Fonteilles & Guitard, 1968) resulting from transmission of a thermal front within the supracrustal sequence. The isotopic results (Marinho, 1991) support and strengthen this interpretation.

The Sete Voltas dome is made up of four representative lithologic units (Martin & Sabaté, 1990; Martin et al., 1991).

- . the oldest rocks are coarse grained tonalitic, trondhjemitic and granodioritic grey gneisses (TTG<sub>1</sub>). They are exposed as large xenoliths within the younger units;
- . the host rocks of these TTG<sub>1</sub> are fine grained grey gneisses (TTG<sub>2</sub>) similar in composition. The rocks are more homogeneous, foliated or sometimes discretely banded;
- . a coarse grained granodiorite with large and abundant feldspar phenocrysts (TTG<sub>3</sub>). This porphyritic granodiorite crops out mainly in the north and center of the dome. It is weakly deformed and the phenocrysts are well preserved away from the NNW-SSE shear zones which cut the dome. On the other hand, in the shear zones and on the borders of the massif, the granodiorite is transformed into augen gneiss. The chronologic field relationship between TTG<sub>2</sub> and TTG<sub>3</sub> is unknown;
- . granitic dykes cut all the previous rocks of the massif. They are grey granites generally weakly deformed but affected by late regional folding.

The isotopic determinations (Martin et al., 1991) yield Rb-Sr whole rock isochron ages of 3.42 Ga for TTG<sub>1</sub> and 3.14, 3.17 Ga for TTG<sub>2</sub> and TTG<sub>3</sub> respectively. Single zircon data of the same rocks corroborate the Rb-Sr ages (see also chapters IV and V), characterizing these as the oldest known rocks in South America.

The grey granite dykes plot on a 2.6 Ga Rb-Sr reference isochron. They are the youngest rocks recognized in the Sete Voltas dome, but their age is not yet firmly established.

Petrographic features are relatively homogeneous on a qualitative point of view. The composition of the rocks vary from trondhjemitic, with less than 10 % K-feldspar and up to 56 % plagioclase, to granodioritic, with 12 to 16 % K-feldspar but with high contents of plagioclase (54 to 65 %). A few samples give a tonalitic composition, containing up to 9 % biotite, whereas some porphyritic rocks have granitic compositions. Plagioclase occurs mainly as phenocrysts or as interstitial crystals between K-feldspar phenocrysts. Biotite is the main mafic phase, but in some of the oldest TTG<sub>1</sub> green hornblende occur associated with biotite. Secondary muscovite occurs in some of the banded grey gneisses related with shear zones.

#### The Boa Vista/Mata Verde Dome

Its tectono-metamorphic history is similar to that of the Sete Voltas dome. This asymmetric dome has a core which presents isotropic or nebulitic structures grading to foliated facies at the border of the dome, where it develops protomylonitic textures. Like in the Sete Voltas dome, the foliation is concordant with the host rock structure. Many amphibolitic xenoliths may occur. The only difference in regard to the Sete Voltas dome is its high microcline content.

Isotopic dating by Rb-Sr and Pb-Pb whole rock and Sm-Nd determinations indicate concordant ages of about 3.4 Ga (Marinho, 1991; see also chapter VI).

#### THE VOLCANO-SEDIMENTARY SEQUENCE

As had been discussed previously the Contendas-Mirante sequence comprises three stratigraphic units (Fig. III.1):

- . lower unit: essentially volcanogenic with some immature sediments;
- . middle unit: epiclastic, pelitic-psammitic;
- . upper unit: epiclastic, meta-arkose with conglomerate layers.

This stratigraphic division, based in Marinho et al. (1979, 1980) and Cunha et al. (1981) incorporates the changes presented recently by Marinho (1991).

#### Lower Unit

The lower unit is subdivided into two formations (Fig. III.1): Jurema-Travessão formation at the base and Barreiro d'Anta formation at the top. The Barra da Estiva road junction subvolcanic body also occur in this lower unit.

#### *Jurema-Travessão Formation*

The rocks of the Jurema-Travessão formation border the Contendas-Mirante belt following the contacts of the lithostratigraphic units of the Jequié and Gavião blocks. Due to folding, they also crop out as a wide antiform in the northwestern tip of the belt. In this latter place, considered as the type-area, the formation comprises metavolcanic rocks (both mafic and felsic) with intercalations of chemical (meta-cherts, marbles and banded iron formations) and detrital metasedimentary rocks. In other regions, mostly in the southern part of the belt, it can be observed a marked change in the lithological composition of the formation: the disappearance of the felsic volcanics and the presence of amphibolites.

#### Meta-Volcanic Rocks

The geochemical signature of these rocks is dominantly tholeiitic (section IIIC), where

the calc-alkaline components are restricted to the felsic volcanoclastic varieties.

Detailed studies carried out in the type area by Cunha et al. (1981), evidenced that these meta-volcanic lithologies are represented essentially by volcanoclastic rocks where the presence of mafic and felsic lavas is subordinated.

#### *Volcanoclastic Rocks*

Several varieties form the volcanoclastic rock group, whose composition range from acid up to basic end members. They present both fine and coarse grain sizes. Basaltic breccias are associated either to these rocks or to the basaltic lavas.

*Meta-tuffs* predominate among the volcanoclastic rocks. Their appearance in outcrop changes according to the composition. They are dark gray, light gray or greenish and are intensely foliated, sometimes microfolded or locally crenulated. They may incorporate some stretched aphanitic lithic material often of basic composition or fragments represented by long quartz aggregates or isolated crystals of plagioclase. The textures are also variable, granolepidoblastic, porphyritic and, sometimes amygdaloidal. Layers of coarse grained acid to intermediate volcanoclastic rocks occur locally, with large amount of fusiform, up to 50 cm long pyroclastic fragments, that sometimes are interpreted as ignimbrites.

*Basaltic breccias* occur either within the meta-tuffs or the amygdaloidal basalts. They are characterized by angular fragments embedded into a fine, schistose matrix of basaltic composition. The fragments of variable size (from grains to blocks) are represented by metabasalts of porphyritic or intersertal texture with corroded plagioclase microphenocrysts in a recrystallized matrix composed of very fine grains of epidote, actinolite needles and scattered plagioclase microliths. The schistose matrix, of the same basaltic nature has intersertal and granolepidoblastic texture; it is similarly composed of plagioclase microliths (An 1-8) scattered among small grains of epidote and actinolite needles, tschermakitic iron-hornblende

to which chlorite flakes are associated. The assemblage is cut by veinlets and clusters of calcite and quartz.

#### *Lavas*

Among the lavas the basaltic types predominate over the felsic ones (acid to intermediate).

The *metabasalts* are of two types, massive and amygdaloidal. The rocks are dark green to dark gray, sometimes light green. They are fine grained or even aphanitic with oriented fabric, often schistose, and always cutted by quartz and carbonate veinlets.

The *massive basalts* have porphyritic, intersertal and granolepidoblastic textures. When the rocks are little tectonized is still possible to recognise plagioclase micropheocrysts or microliths. The matrix is formed by very thin actinolite prisms, Fe-hornblende, Mg-hornblende and ferro-tschermakitic hornblende, plagioclase (An 1-5) and sometimes chlorite flakes.

The *amygdaloidal basalts* present intersertal and amygdaloidal textures. The matrix is very fine grained and formed by plagioclase microliths (An 2-5), actinolite needles and Mg-hornblende, besides small epidote grains. The amygdules are represented by polygonal aggregates of quartz, chlorite and epidote, sometimes in to a radial concentric fabric.

The *felsic lavas* comprise essentially intermediate types with restricted participation of acid types. They are subordinated to their volcanoclastic counterparts. Of gray to greenish colour, they are normally schistose, with quartz and plagioclase phenocrysts up to 4 mm long, their texture is generally porphyritic to intersertal but sometimes lepidoblastic. The plagioclase phenocrysts (An 2-5) are idiomorphic, fragmented and saussuritized, having in some cases microcline-rich nuclei. The quartz phenocrysts are smaller, rounded and with corrosion embayments. The matrix is composed by plagioclase microliths, quartz and Fe-actinolite grains and chlorite flakes.

### Chemical Metasedimentary Rocks

These sedimentary rocks of chemical and chemical-exhalative origin are represented by metacherts, banded iron-formations, marbles and calc-schists closely associated. They form layers of variable thickness from centimeters to meters intercalated among the volcanogenic materials.

*Meta-cherts* - they are massive or banded with very fine grain size. Always recrystallized, they have quartzite or silexite aspect. Their composition ranges from light gray of the essentially quartzose types to dark gray when they are rich in opaque minerals (magnetite or hematite). They are composed essentially by quartz grains and subordinate opaque minerals and chlorite. Scattered grains of pyrite are locally present. Through enrichment in opaque mineral contents the metacherts grade into banded iron formations.

*Banded iron formations* - there are two main types of banded iron-formation, that correspond to the classic "oxide" and "silicate" facies of the literature.

The more common *oxide facies* displays very well defined banding, characterized by the alternance of milimeter thick quartzose and opaque-rich bands. Chlorite, epidote and sericite also occur. Amphiboles of the cummingtonite-grunerite type crystallized where the metamorphic conditions allowed.

The *silicate facies* presents badly developed banding, only visible under the microscope. This banding is marked by fine layers of opaque minerals (magnetite and subordinate ilmenite) into a mass formed by large amphibole crystals of the cummingtonite-grunerite type and, in lesser proportion, of the tremolite-actinolite type. The transition from the oxide to the silicate facies occur through gradual enrichment of amphibole in relation to quartz and opaque minerals.

*Marbles and calc-schists* - the calc-schist consists of discontinuous centimeter thick intercalations within the marbles. They are light greenish grey, sometimes silicified and crosscutted by quartz veins. The marbles form lens-like bodies, generally associated to the metacherts. They are fine grained and massive, with granoblastic texture; are composed of carbonates with some albite, talc and tremolite.

#### Detrital Metasedimentary Rocks

They are abundant and were observed mostly as loose blocks. They are represented by metapelites and metagraywackes. Locally they have aspect of turbidites with wavy bedding and laminations. Among these detrital sediments were also included the pure quartzites associated to metacherts that sustain the relief of the Lajedo range in the center of the antiform located in the NE part of the belt. It is interesting to emphasize the presence of probable detrital zircon and rutile grains within these rocks.

#### *Barreiro D'Anta Formation*

This formation is restricted to the western limb and to the periclinal zone of the Barreiro d'Anta anticline in the NE limit of the Contendas-Mirante belt (Fig. III.1).

The formation comprises an heterogeneous association composed essentially by pyroclastic rocks of acid character with moderately thick intercalations of detrital sediments (metagraywackes and pelites) and chemical-exhalative metasediments (meta-cherts and banded iron formations). These lithologies were not dealt with during the latter years. The available informations are those of Marinho et al. (1979) and Cunha et al. (1981).

#### *Barra da Estiva Road Junction Subvolcanic Body*

This rock body, of rhyolitic composition crops out in the road junction to Barra da Estiva, in the road between Contendas do Sincorá and the village of Pé de Serra. The best place for sampling is a quarry in the northern side of the road, where the rocks are rather fresh.

These rocks are gray coloured and are generally well foliated, and sometimes are cataclastic. They are always very homogeneous, porphyritic with millimetric plagioclase and quartz phenocrysts.

Under the microscope their texture is porphyritic. The plagioclase phenocrysts (An 1-7) are idiomorphic and partially transformed into muscovite and carbonate. The quartz phenocrysts are mostly fragmented and recrystallized, sometimes with corrosion embayments. The recrystallized matrix is represented by a polygonal mosaic of plagioclase and quartz, associated to brown to red-brown biotite and muscovite flakes. The plagioclase phenocrysts nuclei may be transformed into microcline.

#### Middle Unit

The middle unit of the Contendas-Mirante belt is the one with the widest areal extension (Fig. III.1). This clastic assemblage is represented by a thick sequence of metapelites and metagraywackes associated in variable proportions with the predominance of the argillaceous end member. This sequence presents widespread graded bedding and it appears to be similar to a flysch sequence.

It comprises two formations: Rio Gavião formation essentially phyllitic; and Mirante formation, essentially composed of schists. It also includes calc-alkaline volcanic rocks that appear as intercalations within the pelitic rocks.

#### *Mirante and Rio Gavião Formations*

Actually these two formations are different metamorphic grades of the same lithological sequence. The Rio Gavião rocks were metamorphosed in lower temperatures than that of the biotite isograd within the equilibrium domain of the chlorite zone, while the Mirante formation comprises rocks of higher grade.

Their aspect change with the metamorphic grade, from the fine grained, light gray and shining white varieties within the chlorite and

the beginning of the biotite zone, through medium to coarse grained medium gray to dark gray coloured nodulous rocks, in the cordierite zone, up to coarse grained, dark gray to black strongly nodulous rocks within the sillimanite-muscovite and sillimanite-K-feldspar zones. The nodules are poikiloblastic, generally developed after two deformational episodes. However, at some places, such as in the eastern border of the Boa Vista/Mata Verde granitoid, they are affected by the second episode. In this region the anatexis isograd was crossed and the generation of neosomes, in continuous levels or pods parallel to the foliation, lead to the formation of migmatites.

#### Calc-Alkaline Metavolcanic Rocks

These calc-alkaline lithologies were mapped in the NE limit of the belt. They occur intercalated in the schists of the Mirante formation, mostly as basalts, and also crop out as a NE-NW continuous layer that borders the western side of the mafic/ultramafic Rio Jacaré sill, with a predominance of andesitic composition.

The *metabasalts* are massive or amygdaloidal, fine grained, foliated. The amygdules with sizes between 0.1 and 6 mm are sometimes stretched because of the deformation; they are represented by an essentially quartzose polygonal mosaic with a smaller amount of plagioclase. These basalts are composed by amphibole (composition near the limit between Mg and Fe hornblende) sometimes with cummingtonite haloes, plagioclase (An 33-40) and rare opaque minerals (ilmenite and magnetite). When the composition changes towards the andesitic end member, the proportion of amphibole decreases and that of plagioclase increases.

The *andesites* are greenish-gray, foliated, fine grained and often amygdaloidal (amygdules between 0.1 and 1 mm). The presence of dark and rounded spots whose diameter reaches 2 mm is a

characteristic feature of these rocks. Their texture is granolepidoblastic. Amphibole (composition limit between Mg and Fe hornblende), generally oriented clinopyroxene, and a smaller proportion of titanite and zircon are recognized. These minerals are within a granoblastic mosaic of plagioclase (An 31-37) and quartz. The amygdules are formed by quartz and/or plagioclase; sometimes they are infilled by large microcline crystals. The dark rounded spots are made by amphibole aggregates.

#### Upper Unit

This unit coincides with the so called Areião formation (Marinho, 1979) that is the top of the Contendas-Mirante sequence. It contains metarkoses and metasubarkoses; in some places they contain conglomerate layers of variable thickness, with quartz vein and quartzite pebbles and sometimes angular fragments of grayish metapelites.

The rocks are pale gray to buff coloured, fine grained and with decimetric to metric scale cross bedding. The beds of milimetric to decimetric thickness are emphasized by dark layers enriched in magnetite and hematite. Their mineralogy comprises quartz (10-70 %), plagioclase (5-65 %) of albite and oligoclase composition, microcline (0-15 %), sericite (0-20 %) and biotite (0-10 %). In the iron oxide-bearing horizons, the opaque minerals can reach concentrations of up to 50 %.

It is important to stress the difference between the sedimentation regimes of the middle and upper units:

- . middle unit: flysch type with frequent graded bedding;
- . upper unit: continental-fluvio-deltaic, platformal.

This contrast in the depositional

environment suggests a discontinuity between these two units. The presence of such discontinuity is strengthened by the isotopic data (chapter IV).

### THE INTRUSIVE ROCKS

In this section are included the following plutons (Fig. III.2):

- . Lagoa do Morro granitoid (*sensu lato*);
- . Pé de Serra granite;
- . Rio Jacaré sill;
- . The Transamazonian granites.

#### The Lagoa do Morro Granitoid (*Sensu Lato*)

This granitoid was considered by Marinho et al. (1980), Marinho & Sabaté (1982) and Cordani et al. (1985) as the reference massif for all the augen granitoids of the southwestern part of the Contendas-Mirante belt. This procedure was based mostly in the common macroscopic aspects of these bodies.

Marinho (1991) indicated the existence of three independent bodies (Fig. III.2) with distinct petrographic and geochemical features. These bodies were designated Lagoa do Morro *sensu stricto*, Serra dos Pombos and Pau de Colher granitoids.

#### The Lagoa do Morro Granitoid (*Sensu Stricto*)

The type-region of this granitoid is the Lagoa do Morro farm where it crops out in wide slabs. The rocks are light gray to pinkish gray, fine grained and generally foliated with feldspar megacrysts up to 4 cm long.

Under the microscope, microcline phenocrysts that include saussuritized plagioclase (An 15-17), within a fine grained (0.5-1 mm) polygonal mosaic made up of microcline, plagioclase and quartz occur. The mosaic still

comprises green to pale brown biotite crystals oriented and closely associated to epidote, allanite and titanite crystals. It is observed a tendency of quartz to segregate in bands parallel to the foliation delineated by biotite. These rocks are often cut by quartz, pegmatite and fine grained granite veins.

#### The Serra dos Pombos Granitoid

The type-area of this granitoid is found in the Pombos range in the road BA-262, between the towns of Vitória da Conquista and Anagé. In this region occur numerous meter-sized schist enclaves within the granitic rocks.

The granitoids are light gray coloured, medium grained, foliated and have large feldspar megacrysts up to 3 cm long. Locally they are cut by pegmatite and fine grained granites.

The microcline megacrysts enclose and assimilate saussuritized plagioclase grains (An 13-15). They are disposed within a mosaic formed by plagioclase (also saussuritized), quartz and microcline. Red to pale-brown biotite associated to muscovite is oriented according to a sharp foliation. Quartz also appears in clusters probably as a product of remobilization.

The following characteristics distinguish the Serra dos Pombos granitoid from the Lagoa do Morro one:

- . absence of quartz segregation into bands;
- . the biotite type;
- . the presence of muscovite;
- . the absence of allanite and smaller amounts of titanite.

#### Anagé/Pau de Colher Granitoid

It corresponds to the westwards concave curved band that borders the SW end of the Contendas-Mirante belt, nearby the Anagé town.

In the northern end of the band, in the

place named Pau de Colher, occur fine grained gneissic enclaves. These enclaves appear to be similar to metagraywackes of the Contendas-Mirante middle unit, but there is no confirmation of this so far.

The granitic rocks are pinkish, coarse to medium grained, often they have K-feldspar megacrysts up to 5 cm long augen-shaped or as disordered hypidiomorphic grains. The texture is generally mylonitic. Plagioclase phenoclasts of several dimensions are recognized, surrounded by muscovite and reddish brown biotite, within a fine grained polygonal matrix. This matrix is composed by plagioclase and quartz that form a vein net.

### **Pé de Serra Granite**

This granite forms a NE-SW stretched band about 100 km long and 5 km of maximum width cropping out along the northeastern border of the Contendas-Mirante belt (Fig. III.2). It comprises alkaline and sub-alkaline rocks.

### *Sub-Alkaline Rocks*

The sub-alkaline rocks represent almost all lithologies of this granitic belt. They are pinkish-light gray to buff, fine grained and sometimes banded. The main foliation, parallel to this banding is deformed by the normal folds of the second main deformational episode that also affects the volcano-sedimentary sequence.

Their texture is oriented granoblastic, represented by a fine grained (0-0.5 mm) mosaic composed by saussuritized plagioclase (An 17-20), clear microcline and quartz with anhedral to subhedral bluish-gray to pale reddish-brown (magnesium-hastingsitic hornblende type) amphibole associated to abundant titanite crystals. In some samples occur large saussuritized plagioclase crystals sometimes elongated and with Carlsbad-albite twinning.

In some places of the granitic band, the rocks are finer grained with a very fine grained (0.05-0.1 mm) mosaic and relict crystals of

plagioclase and microcline up to 0.5 mm long. These finer grained varieties are richer in green biotite and epidote.

### *Alkaline Rocks*

This group encompasses alkaline granites and syenites with aegirine and andradite. Such varieties are associated to the essentially sub-alkaline band that forms the Pé de Serra granite as well as to the plutonic and supracrustal rocks of the granulitic belt. Within the band its relationships with the sub-alkaline rocks were not determined. Inside the granulitic belt they appear as small elongated bodies (< 3x0.5 km) that appear to be intrusive.

The rocks are light-gray coloured, fine grained and foliated. Their texture is heterogranular hypidiomorphic and sometimes protomylonitic. Aegerine crystals, sometimes oriented, commonly associated to andradite and titanite, within a medium grained (0.7-2 mm) mosaic essentially composed of albite (An 1-2) in hypidiomorphic grains with exsolutions of K-feldspar. Also in this mosaic the abundant presence of microcline, and subordinate presence of quartz, is recorded.

The hypidiomorphic texture displayed by these alkaline rocks suggests that they have been subjected to a deformational history gentler than the one that affected the sub-alkaline lithologies. The isotopic data (chapter IV) indicates that these alkaline rocks are younger than the sub-alkaline ones.

### **The Rio Jacaré Sill**

This sill is a NE oriented band about 40 km long and with an average width of 1 km occurring near the eastern border of the Contendas-Mirante belt (Figs. III.1 and III.2), between the calc-alkaline rocks of the middle unit of the Contendas-Mirante sequence to the west, and the Pé de Serra granite to the east.

It was first mapped by Galvão et al. (1981) and has vanadium deposits associated to

magnetite-rich bodies whose average  $V_2O_5$  concentration is 2%; the measured reserves are 150,000 tons of  $V_2O_5$ .

A more detailed stratigraphic and petrographic study of the sill was carried out by Brito (1984); he described a lower zone essentially composed by gabbros and an upper stratified zone where cyclically repeated gabbros, pyroxenites, and magnetites occur.

Marinho (1991) attempted to determine the isotopic signature of this lithological unit and check the cogenetic nature of the studied samples using geochemical data (major and trace elements including rare earths). The sampling was focused on the gabbroic facies, always using drill cores.

The gabbros are somewhat dark coloured according to the relative proportion of plagioclase and mafic minerals. The prevalent types are medium to coarse grained, well foliated. There are two distinguishable types of texture that are sometimes associated in thin section. These textures are related to different degrees of intensity in the deformation/recrystallization processes.

. In the less affected rocks, the plutonic intersertal texture is still preserved. In this case large (up to 5 mm) plagioclase phenocrysts (An 45-52) commonly saussuritized can be observed, in whose interstices are concentrated opaque minerals and bluish-green amphiboles (Fe-hornblende type), with inclusions of small crystals of Fe-tschermakitic hornblende. Relicts of clinopyroxene are found in the nucleus of some amphibole crystals, that commonly are associated to small titanite grains and quartz droplets. Some grains of opaque minerals with titanite aureoles are observed inside the amphibole crystals.

. The increase in the intensity of the recrystallization/deformation processes proceed through textures in which relict plagioclase phenocrysts survive within a

polygonal mosaic, finally reaching typical granonematoblastic textures. Such textures are characterized by actinolitic and Fe-actinolitic hornblende crystals that generally are oriented and sometimes have inclusions of Mg-hornblende small idiomorphic grains inside a plagioclase (An 35-40) and quartz polygonal mosaic (0.5 mm). The garnet (Al = 78; Py = 4; Sp = 4; Gr = 14) when present can both integrate the mosaic and form either sin-helictic or post-tectonic porphyroblasts up to 5 mm long. The brown to pale red-brown biotite is always associated to the amphibole and the opaque minerals. These are represented by large magnetite or titanite crystals and by ilmenite flakes. In the case of rocks with preserved plutonic textures, the opaque minerals occupy the spaces between the plagioclase phenocrysts.

### **The Transamazonian Granites**

The axial zone of the Contendas-Mirante belt and its contact interface with the adjacent terrains are underlined by several granitic bodies. These belong to the alignment of peraluminous intrusions which delineates the N-S, up to 500 km long, Jacobina-Contendas orogenic domain (Sabaté et al., 1990a, b) corresponding to the limit between the granulitic terrains of the Jequié block and the medium-grade terrains of the Gavião block in the central part of the São Francisco craton (Fig. III.3).

In the Contendas-Mirante belt, the granitic plutons are generally elongated. Their emplacement, along or parallel to the major structures is syn- to post-tectonic to the late regional deformation which corresponds to the E-W shortening of the belt; it is accompanied by folding and vertical shear-zones (Sabaté et al., 1980, see also below). Several bodies were recognized (Marinho et al., 1979, 1980; Petta, 1979) and their emplacement mechanism was discussed (Marinho & Sabaté, 1982). In the southern part of the belt, Conceição (1986) shows

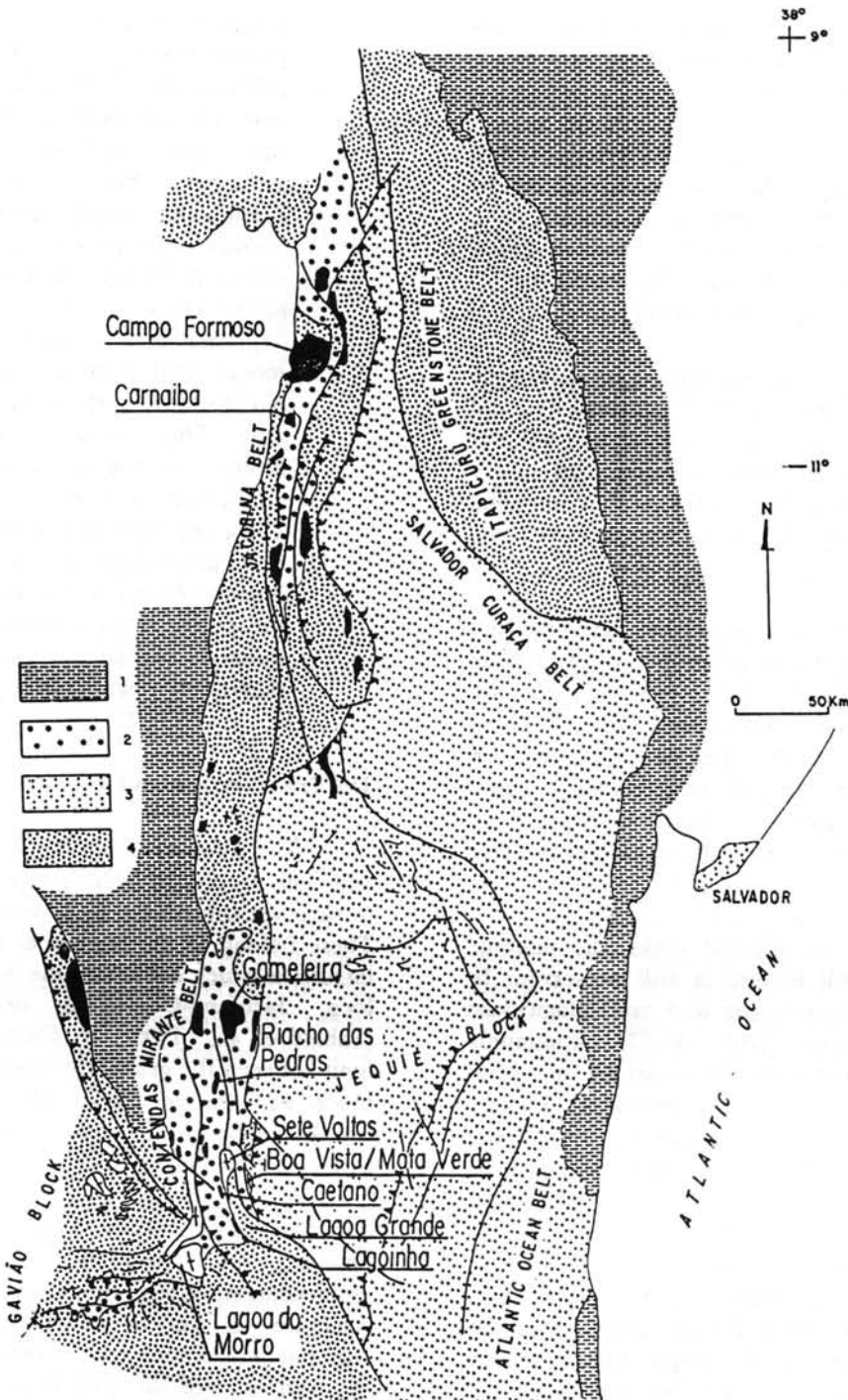


Figure III.3 - Tectonic sketch map of the Gavião block and Jequié block junction zone. Location of the studied intrusions in relation to the main structures. 1. Phanerozoic and Middle and Late Proterozoic covers and belts; 2. volcano-sedimentary belts; 3. high-grade terrains: Jequié block granulitic formations and Archean to Early Proterozoic mobile belts; 4. Gavião block medium-grade formations; dark - late- to post-tectonic Transamazonian granitoids; cross - older (Archean) and syn-tectonic (Early Transamazonian event) plutons.

the succession of the intrusions relative to deformation and correlates them with the degree of differentiation from the southernmost biotite rich granite (deformed under sub-solidus conditions) to the northernmost and undeformed muscovite-rich granite.

In agreement with the relative ages of emplacement, the Rb-Sr isotopic ages yielded an interval of 1974-1929 Ma from the earliest (Lagoinha/Lagoa Grande syn-kinematic pluton) to the latest (Riacho das Pedras post-kinematic) through an intermediate late-kinematic (Gameleira pluton) with an age of 1947 Ma (Sabaté et al., 1990; Marinho, 1991).

#### *Emplacement and Petrographic Description*

All granites intrude the supracrustal rocks and some of them can be emplaced close to the Archean domes due to the tectonic discontinuities which control its emplacement. These granites show an homogeneous aspect and correspond to equigranular, fine to medium grained, biotite-poor two-mica leucogranite, with variable amounts of muscovite (Cuney et al., 1990).

From south to north, the Lagoinha and the Lagoa Grande plutons are elongated parallel to the tectonic contact which limits the Archean Sete Voltas dome to the east and the supracrustal rocks of the belt. The former contains biotite or muscovite-rich schlieren and muscovite-biotite-tourmaline pegmatitic pockets, aligned to the ductile vertical foliation. In the latter, the magmatic fabric of the homogeneous biotite granite is underlined by biotite-garnet schlieren parallel to the elongation of the body and the regional foliation trend of the surrounding rocks. A parallel ductile deformation is superposed to the magmatic flow of both plutons, increasing eastwards to mylonitic texture on its eastern margins.

The Caetano and Aliança plutons belong to the same intrusion and form two elongated bodies intruding the Mirante schists. They are composed of a fine grained homogeneous two-mica-garnet leucogranite with muscovite-rich uraninite layers, biotite + garnet schlieren and

with muscovite + biotite + garnet + tourmaline pegmatites, roughly aligned along the magmatic foliation.

The northern Riacho das Pedras pluton is clearly post-tectonic, with typical magmatic stopping features in the Mirante schists where a contact metamorphism is induced. It is composed by a leucocratic garnet-bearing two-mica granite with abundant muscovite. In the northeastern part of the belt, the Gameleira pluton represents the largest biotite-rich two-mica leucogranitic intrusion. It emplaced into the core of an open antiformal dome during the last regional deformational episode and is responsible for the deviation of the andalusite/cordierite isograd of the regional transamazonian metamorphism.

#### *Mineralogic Description*

On the scale of the whole belt, the average proportion of quartz and plagioclase, and its anorthite content, show variations which are not correlated with the geographic position or the chronologic distribution. The earliest two intrusions, Lagoinha and Lagoa Grande, mark the lower and higher An contents of all other leucogranites, including the Jacobina belt intrusions. The Riacho das Pedras granite differs by its richness in albite (Cuney et al., 1990).

The biotite proportion is always less than 7% and its aluminium and magnesium contents are slightly lower and higher, respectively, in comparison with the European paleozoic peraluminous leucogranites (Cuney et al., 1990).

Muscovite content vary widely from 1 to 14%. As for plagioclase and quartz, the Lagoinha and Lagoa Grande intrusions mark the higher and lower values, respectively. Two types of muscovite are observed: (i) an euhedral primary muscovite which is the more abundant; (ii) secondary muscovite which may have several habits (Cuney et al., 1990).

A weak chloritization may appear in most of the granites. Apatite, zircon and allanite are the common accessory minerals together with magnetite. Uraninite is clearly present in the

Aliança pluton and large monazite crystals may be found in the Riacho das Pedras granite (Cuney et al., 1990).

## GEOCHEMICAL CHARACTERIZATION

In this brief item the geochemical characterization of the several outcropping units of the Contendas-Mirante belt will follow whenever possible the same division used to describe their geological setting. Most data are from Marinho (1991) but some are from Cuney (1990) and Martin et al. (1991).

### THE BASEMENT DOMES

#### The Sete Voltas Dome

In the Sete Voltas dome, both TTG<sub>2</sub> and TTG<sub>3</sub> show typical Archean characteristics (Martin & Sabaté, 1990; Martin et al., 1991, 1992). They have low K<sub>2</sub>O/Na<sub>2</sub>O ratios, follow trondhjemitic trends of differentiation on a K-Na-Ca triangle (Fig. III.4) and display highly fractionated REE patterns and strong Ytterbium depletion (Fig. III.5).

Their Sr isotopic composition, with low initial <sup>87</sup>Sr/<sup>86</sup>Sr (Sr<sub>i</sub>) close to 0.702 precludes a crustal origin and rather militates in favour of a direct or indirect mantle origin. In addition, the REE patterns and major element distribution allowed Martin et al. (unpublished results) to propose a classical two stage petrogenetic model for these rocks: (1) partial melting of the mantle gave rise to tholeiites; (2) the latter, transformed into garnet-bearing amphibolite, underwent melting thus generating the TTG association.

The TTG<sub>1</sub> rocks show peculiar features. For instance, they are strongly depleted in K<sub>2</sub>O with a K<sub>2</sub>O/Na<sub>2</sub>O ratio extremely low (0.3). Their REE are also highly fractionated but seem to be more HREE depleted than TTG<sub>2</sub> or TTG<sub>3</sub>, their Sr<sub>i</sub> = 0.6997 is very low and mantle derived compatible (Martin et al., 1991, 1992 and unpublished results). These authors suggest that the source composition of TTG<sub>1</sub> may be distinct

or that the petrogenetic processes were sensibly different in the Early Archean (3.4 - 3.1 Ga) from those known in the Late Archean (2.9 - 2.5 Ga).

#### The Boa Vista/Mata Verde Dome

As seen above, the Boa Vista/Mata Verde dome associates predominantly tonalite-trondhjemitic rocks with microcline rich granodiorite terms. The compositions are similar to those defined by Barker (1979), with the exception of the FeO and MgO contents which are different from those of classic trondhjemites. Both a trondhjemitic and a calc-alkaline trend are found (Fig. III.4).

The REE patterns are less fractionated than in the late Archean TTG (Martin, 1986) without the typical concavity of the HREE (Fig. III.5). A weak negative Eu anomaly appears (Marinho, 1991). This pattern is similar to those of some phenocryst granodiorite of the Sete Voltas dome (Martin et al., unpublished results).

In opposition to the Sete Voltas lithologic equivalents, the Boa Vista/Mata Verde rocks show two distinct geochemical groups, related with TTG and calc-alkaline plutonic associations, respectively. Fractional crystallization appears to be responsible for most of the evolution (Marinho, 1991). Sr and Nd isotopic data with Sr<sub>i</sub> = 0.7008 and ε<sub>Nd</sub> = -0.8 to 0.2, support a similar petrogenetic model to that proposed for the Sete Voltas TTG<sub>2</sub> and TTG<sub>3</sub> associations but with a probable crustal contribution (Marinho, 1991).

### VOLCANO-SEDIMENTARY SEQUENCE

Only the geochemical signatures of volcanic rocks will be discussed with the aim of characterizing their magmatic series and their probable tectonic setting, whenever possible.

Marinho (1991) demonstrated for the first time the bimodal character of the Contendas-Mirante sequence volcanism, evidencing the existence of a tholeiitic series in the NW part of the belt and a calc-alkaline series in its NE part.

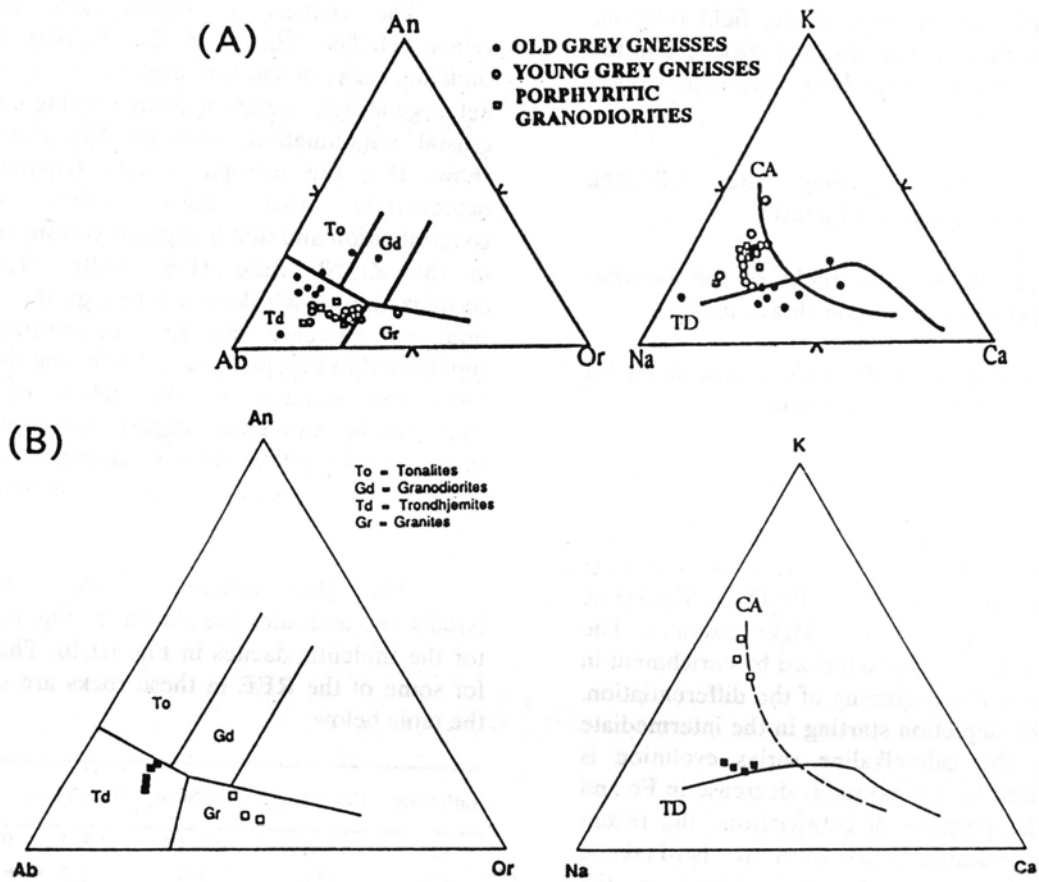


Figure III.4 - Normative An-Ab-Or and K-Na-Ca diagrams for Sete Voltas (A) and Boa Vista/Mata Verde (B) granitoids (After Cuney et al., 1990 and Marinho, 1991).

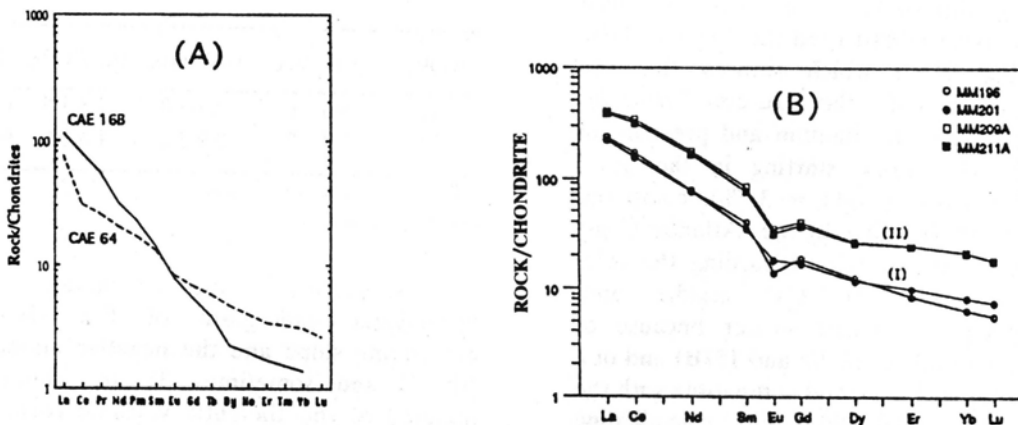


Figure III.5 - REE patterns of granitoid rocks: (A) Sete Voltas massif; (B) Boa Vista/Mata Verde (I) and Lagoa do Morro (II) (after Cuney et al., 1990 and Marinho, 1991).

The isotopic data as well as the field relations have shown that the calc-alkaline rocks are in the middle unit and not in the lower one as previously assumed.

The data regarding the following lithologies will be discussed jointly:

- . tholeiitic volcanic rocks of the Jurema-Travessão formation (lower unit);
- . sub-volcanic body of the Barra da Estiva road junction (lower unit);
- . calc-alkaline volcanic rocks (middle unit).

Marinho (1991) shows that the discrimination between the tholeiitic and calc-alkaline series is sharp in the  $Fe_2O_3$  vs MgO (Fig. III.6) and  $TiO_2$  vs  $FeO^+/MgO$  diagrams. The tholeiitic series is characterized by enrichment in Fe and Ti in the beginning of the differentiation, followed by depletion starting in the intermediate members; the calc-alkaline series evolution is characterized by a continuous decrease in Fe and Ti. For the purpose of comparison the recent island arc volcanic series from the Isu-Hakone volcano of Japan were also plotted in the diagrams. There is a relatively good agreement between the trends of the tholeiitic and calc-alkaline series of the Contendas-Mirante belt and those of these Japanese volcanics.

Trying to compare the Contendas-Mirante series (CM) with those of the "Atlantic Coast Domain" Barbosa (1986) used the MgO vs  $TiO_2$  diagram (Fig. III.7) which showed that the tholeiitic series of the Jurema-Travessão Formation is richer in titanium and presents an inversion of the trend, starting in the more developed members ( $MgO = 3\%$ ), compared with that of the tholeiites of the "Atlantic Coast Domain" (see Chapter II). Regarding the calc-alkaline series of the CM middle unit, notwithstanding a stronger scatter because of volcanoclastic samples (18, 98 and 151B) and of a metasomatized rock, a trend compatible with the evolution of the Atlantic Coast calc-alkaline series is found.

The changes in incompatible element ratios (Th/Nb, Th/Zr, Y/Zr, Zr/Nb), in the tholeiitic rocks of the CM may be due to mantle heterogeneities, variation in the melting ratios or crustal contamination. However, Marinho (1991) shows that the isotopic results (chapter IV) demonstrate that there exists crustal contamination and that it explains certain changes in the Zr/Nb ratio (Fig. III.8). Fractional crystallization which does not change the Zr/Nb ratio but increase the Zr concentration is superposed to that process. Also for the tholeiitic rocks the changes in the ratios of these incompatible elements suggest heterogeneities that could be either directly connected to the source or produced during a contamination process.

The REE patterns for the tholeiitic basalts and andesites are shown in Fig. III.9 and for the tholeiitic dacites in Fig. III.10. The ratios for some of the REE in these rocks are show in the table below:

Lithology	(La/Yb) <sub>N</sub>	(La/Sm) <sub>N</sub>	(Gd/Yb) <sub>N</sub>	Eu/Eu*
(1)	5.6-8.1	2.1-3.1	1.8-2.4	0.94-1.18
(2)	13.6	3.7	2.2	0.71

(1) Basalts and basaltic andesites

(2) Tholeiitic dacites

The REE patterns of the calc-alkaline rocks are shown in Fig. III.11 and their REE ratios in the following table:

Lithology	(La/Yb) <sub>N</sub>	(La/Sm) <sub>N</sub>	(Gd/Yb) <sub>N</sub>	Eu/Eu*
(1)	5.6-7.0	2.3-3.0	1.3-1.8	0.80-0.96
(2)	6.7-7.9	2.9-3.2	1.6-1.8	0.49-0.61

(1) Basalts and basaltic andesites

(2) Tholeiitic dacites

Concerning the primitive mantle normalized spidergram of Fig. III.12, the descending slope and the negative anomalies in Nb, P and sometimes Ti are characteristic features of the tholeiitic volcanic rocks of the Jurema-Travessão Formation. These patterns are compatible with those of continental tholeiites. It

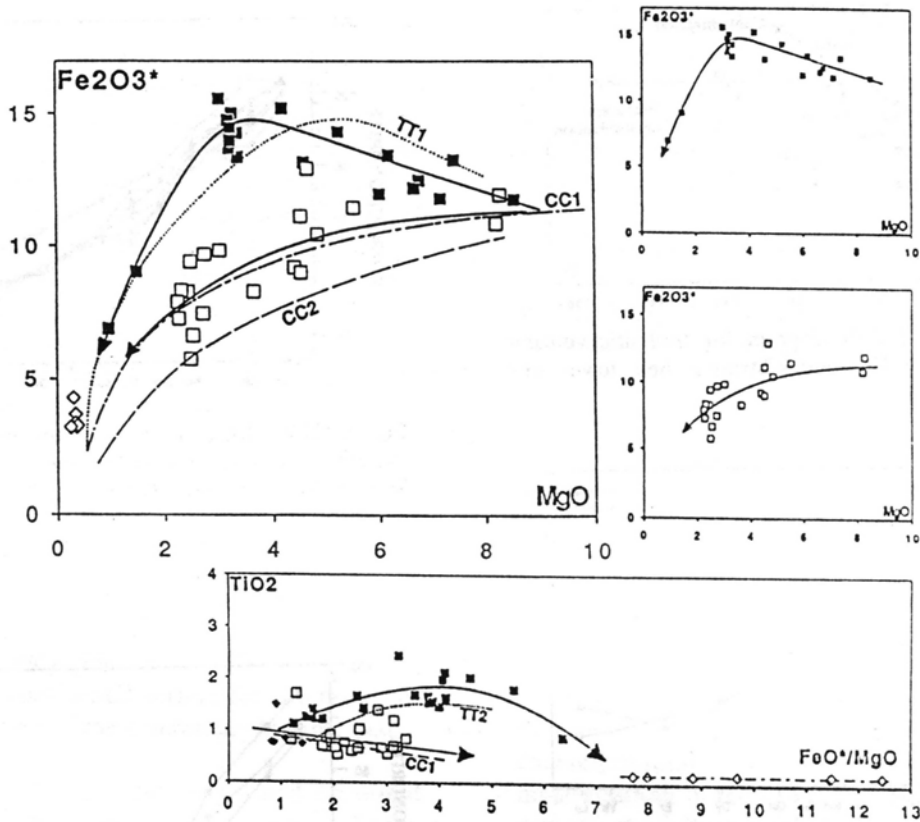


Figure III.6 -  $\text{Fe}_2\text{O}_3^*$ -MgO and  $\text{TiO}_2$ -( $\text{FeO}^*/\text{MgO}$ ) diagrams showing the distinction between the tholeiitic lower unit (■) and calc-alkaline middle unit (□) volcanic rocks of the Contendas-Mirante volcano-sedimentary sequence. (◇) Barra da Estiva road junction sub-volcanic rocks; (TT1) and (CC1) tholeiitic and calc-alkaline series from Isu-Hakone volcano (Kuno, 1954); (TT2) = tholeiitic series from Miyake-Jima volcano (Miyashiro, 1973); (after Marinho, 1991).

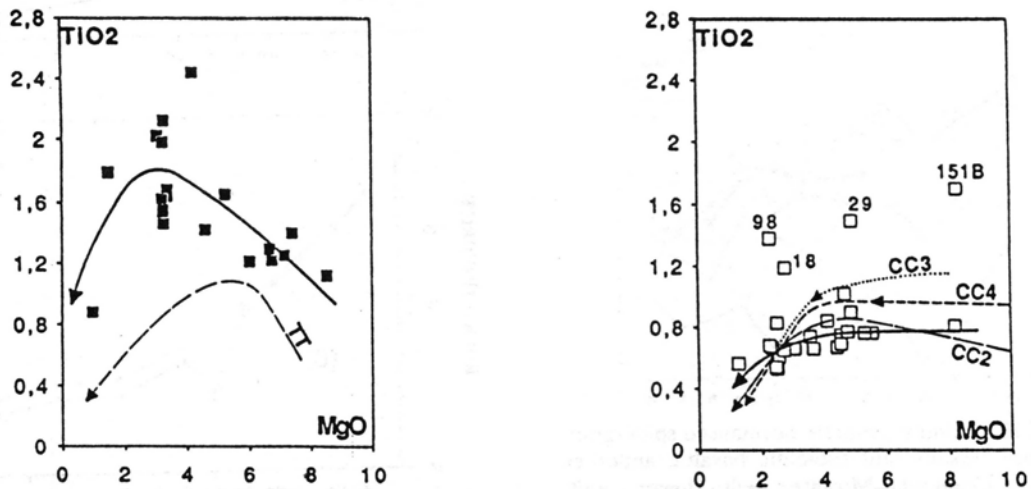


Figure III.7 - MgO-TiO<sub>2</sub> diagram for the tholeiitic lower unit (■) and calc-alkaline middle unit (□) volcanic rocks of the Contendas-Mirante volcano-sedimentary sequence. (TT) and (CC2) = tholeiitic and calc-alkaline series from Atlantic Coast Domain; (CC3) = calc-alkaline series from Chile (Déruelle, 1979); (CC4) = basic rocks and calc-alkaline granites from Ansignan and Cassagnes (Fontelles, 1976); (after Marinho, 1991).

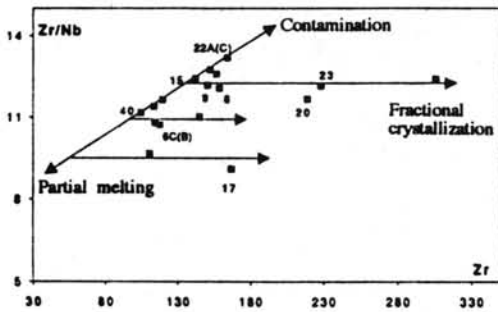


Figure III.8 - Zr/Nb diagram for tholeiitic volcanic rocks from the Contendas-Mirante belt lower unit (Marinho, 1991).

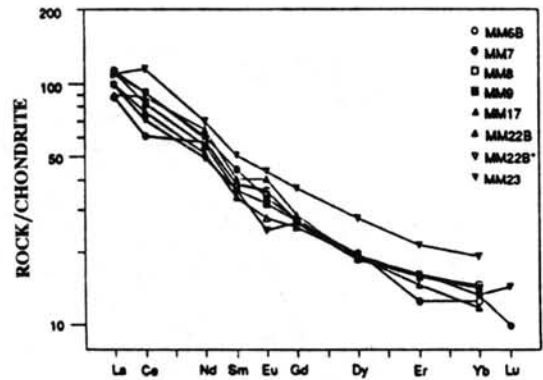


Figure III.9 - REE patterns of tholeiitic basalts and tholeiitic basaltic andesites from the Contendas-Mirante belt lower unit (Marinho, 1991).

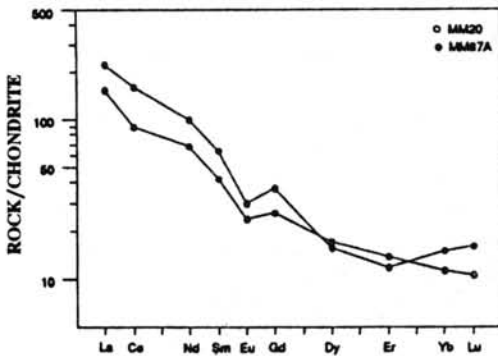


Figure III.10 - REE patterns of tholeiitic dacites (MM20) and Barra da Estiva road junction sub-volcanic rocks (MM87A) from the Contendas-Mirante belt lower unit (Marinho, 1991)

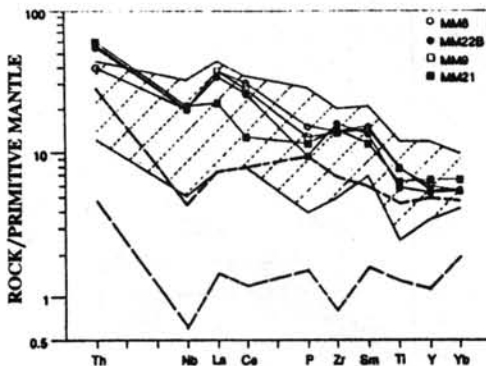


Figure III.12 - Primitive mantle normalised spidergram for tholeiitic basalts and tholeiitic basaltic andesites from the Contendas-Mirante belt lower unit. Normalising values after Holm (1985). The hatched zone limits the continental tholeiitic field. The continental margin arc tholeiitic field is limited by the two stippled lines (after Marinho, 1991).

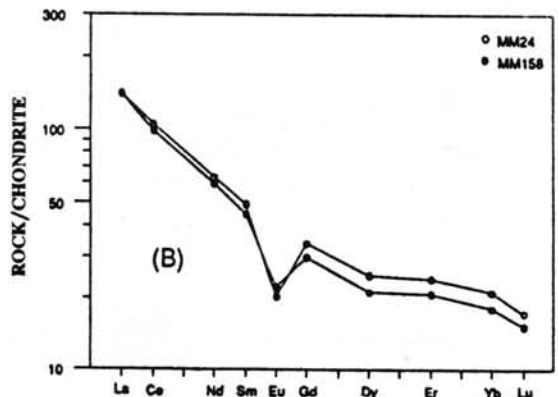
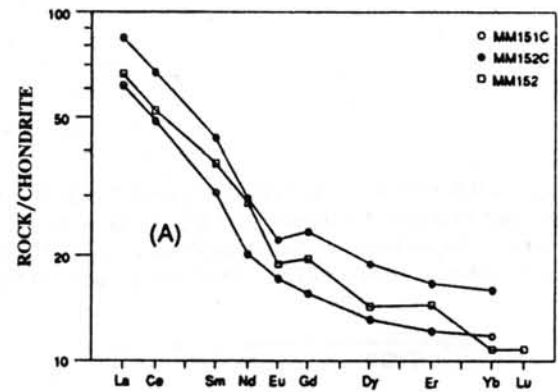


Figure III.11 - REE patterns of Contendas-Mirante middle unit calc-alkaline volcanic rocks: (A) basalts and basaltic andesites; (b) andesites (after Marinho, 1991).

is distinguished from the E-MORB patterns by the absence of positive Nb anomalies. The presence of negative anomalies of Nb, P and Ti as well as the common presence of andesitic members could lead to a comparison of these tholeiitic volcanic rocks to continental margin tholeiites. Trying to clear this doubt, Fig. III.12 shows the field of basalts and basaltic andesites of this environment, where it can be observed that the declivity of this field (hatched zone in the figure) is approximately nil and that the average concentration of each element is, at least four times smaller than in our tholeiites. The significant participation of the andesitic members is in agreement with the crustal contamination previously discussed.

It is important to emphasize that the geotectonic discrimination diagrams of Pearce and Cann (1973), Pearce et al. (1977) and Meschede (1986) (Figs. III.13, III.14 and III.15) also show a continental setting for the tholeiites of the lower unit of the Contendas-Mirante belt.

The Zr/Y ratios between 4 and 7.5 would characterize the calc-alkaline rocks of the Contendas-Mirante belt middle unit as continental arc volcanism (Pearce and Norry, 1979).

With regard to the magmatic processes that generated the tholeiitic (lower unit) and calc-alkaline (middle unit) volcanic series of the Contendas-Mirante belt, the Ni vs Th diagram (Fig. III.16) shows the clearly compatible character of Ni along the differentiation, suggesting that fractional crystallization played an important role during the evolutive process.

The geochemical characterization of the sub-volcanic body of the Barra da Estiva road junction is problematic. With its average content of SiO<sub>2</sub> (about 77 %) these rocks are extremely evolved. As there are no less differentiated members it is a difficult task to characterize the magma that gave origin to these lithologies. Even if it is assumed that such lithologies are one of the most evolved products of the magma that generated the volcanic series previously discussed, the immediate solution of the problem

will not be found. This is because the points that represent the compositions of the Barra da Estiva road junction rocks in the diagrams used (Figs. III.6 and III.7) plot in the end of the differentiation curves, exactly in the sector where the tholeiitic and calc-alkaline series converge.

Fig. III.10 shows the REE spectrum of only one sample of this sub-volcanic body that was analysed. The spectrum is fractionated with the following characteristics:

(La/Yb) <sub>N</sub>	(La/Sm) <sub>N</sub>	(Gd/Yb) <sub>N</sub>	Eu/Eu*
14.9	3.6	2.4	0.59

#### THE INTRUSIVE ROCKS

A summary of the study carried out by Marinho (1991) for the geochemical characterization of the several plutonic manifestations of the Contendas-Mirante belt will consider the following lithologies:

- . Lagoa do Morro granitoid (*sensu lato*);
- . Pé de Serra granite;
- . Rio Jacaré sill;
- . Transamazonian granites.

#### Lagoa do Morro Granitoid (*Sensu Lato*)

The geochemical study of this granitoid included only the Lagoa do Morro (*sensu stricto*) and Serra dos Pombos massifs. This study was based in very few samples: seven for the former and two for the latter.

The transitional peraluminous/metaluminous character of the Lagoa do Morro (s.s.) pluton is evidenced by the [Al - (Na + K + 2Ca)] vs [Fe + Mg + Ti] diagram (Debon and Le Fort, 1988; Fig. III.17). Regarding the Serra dos Pombos massif, the plot of the two samples

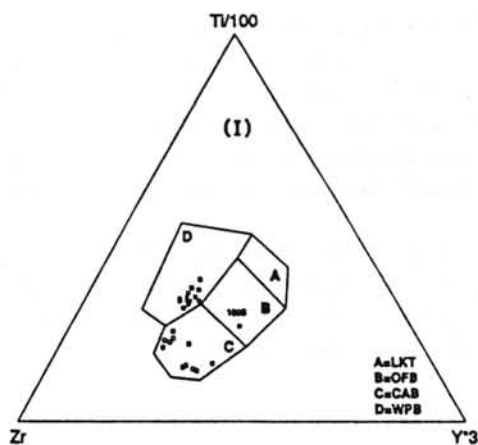


Figure III.13 - Pearce & Cann (1973) geotectonic diagram for the Contendas-Mirante volcanic rocks: (●) = lower unit tholeiitic rocks; (□) = middle unit calc-alkaline rocks. All those samples satisfy the condition  $12 < (CaO + MgO) < 20\%$  (after Marinho, 1991).

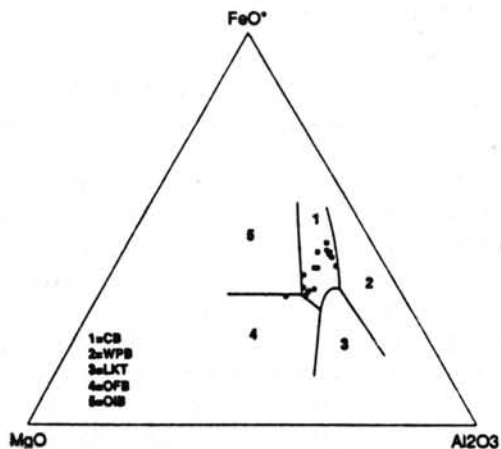


Figure III.14 - Pearce et al. (1977) geotectonic diagram for the Contendas-Mirante lower unit tholeiitic rocks. All those samples satisfy the condition  $51 < SiO_2 < 56\%$  (after Marinho, 1991).

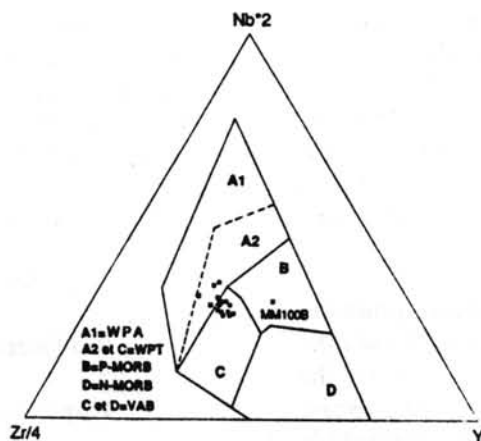


Figure III.15 - Meschede (1986) geotectonic diagram for the Contendas-Mirante lower unit tholeiitic rocks. All those samples satisfy the condition  $12 < (CaO + MgO) < 20\%$  (after Marinho, 1991).

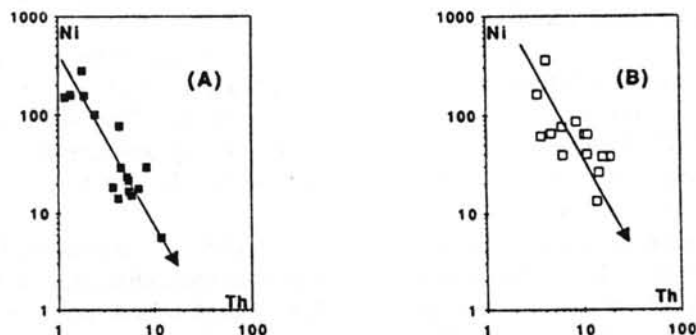


Figure III.16 - Ni-Th diagram for the tholeiitic lower unit (A) and calc-alkaline middle unit (B) volcanic rocks of the Contendas-Mirante sequence (after Marinho, 1991).

suggests its peraluminous character.

The study of the changes of trace elements shows a compatible behaviour for most of them, except for Th and Rb, clearly incompatible. Thus Rb was chosen as differentiation index since Th does not present enough variation and the accuracy of its determination is uncertain. Fig. III.18 shows that the two granitoids are clearly individualized.

REE analyses of two samples of the Lagoa do Morro (s.s.) granitoid reveal similar fractionated patterns (Fig. III.5), with Eu negative anomalies:

Sample	(La/Yb) <sub>N</sub>	(La/Sm) <sub>N</sub>	(Gd/Yb) <sub>N</sub>	Eu/Eu*
209A	19.21	4.94	1.86	0.57
211A	18.08	5.08	1.76	0.55

These spectra are parallel to those of the Boa Vista/Mata Verde rocks, although with slightly higher concentrations, e.g. La = 200 times chondrite to Boa Vista/Mata Verde and 400 times chondrite for Lagoa do Morro.

In the same way that for the Boa Vista/Mata verde granitoid, among the partial melting, mixture, and fractional crystallization petrogenetic processes, the latter looks to be the better suited to explain the geochemical variations. A distinction between the Lagoa do Morro and Serra dos Pombos massifs, that will be seen again in the isotopic geochronology/geochemistry evaluation (Chapter IV), appears to indicate a different process for the latter.

### The Pé de Serra Granite

The geochemical study of the Pé de Serra granite was also based in a small number of samples: seven of the sub-alkaline rocks and two of the alkaline lithologies. The characterization of the petrogenetic evolution as well as the relationships between the two facies is difficult

due to the small number of samples. Nevertheless, there are interesting aspects to take into consideration.

Figs. III.19 to III.21 clearly separate the amphibole bearing sub-alkaline rocks from the aegirine and andradite bearing alkaline rocks. The [Al/(K + Na + 2Ca)] vs TiO<sub>2</sub> diagram (Fig. III.19) also evidences the metaluminous character [Al/(K + Na + 2Ca) < 1] of these two facies (see chapter IV).

For the sub-alkaline rocks the study of the fractionation of the major elements show that the contents of these elements decrease with differentiation, except for K<sub>2</sub>O that is constant in the beginning of the process and increases in the end of it. Regarding the trace elements it is clear that only Sr presents a compatible character; the others are incompatible and their concentrations increase variably with the magmatic evolution.

The ratios between K, Rb, Sr and Ba are presented in the following table:

K/Rb	Rb/Sr	Ba/Sr
250-200	0.85-3	4.5-13

Fig. III.22 shows two REE patterns, one for the sub-alkaline rocks (MM 32A) and the other for the alkaline rocks (MM 163). Though they are similar, both highly fractionated with negative Eu anomalies, the one for the alkaline rocks is richer in REE, more fractionated and with a stronger fractionation for the LREE:

Sample	(La/Yb) <sub>N</sub>	(La/Sm) <sub>N</sub>	(Gd/Yb) <sub>N</sub>	Eu/Eu*
32A	5.45	3.21	1.19	0.64
163	6.98	3.70	1.21	0.57

These patterns are very different from those of the Boa Vista/Mata Verde and Lagoa do Morro granitoids and are comparable to the patterns of the charnockitic rocks of Maracás region (Chapter II).

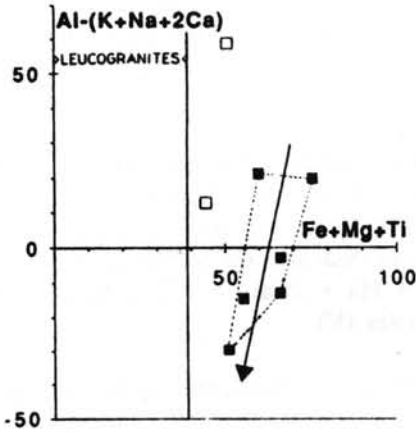


Figure III.17 - Debon & Le Fort (1988) (Al-Na-K-2Ca)-(Fe+Mg+Ti) diagram for Lagoa do Morro (■) and Serra dos Pombos (□) granitoids (after Marinho, 1991).

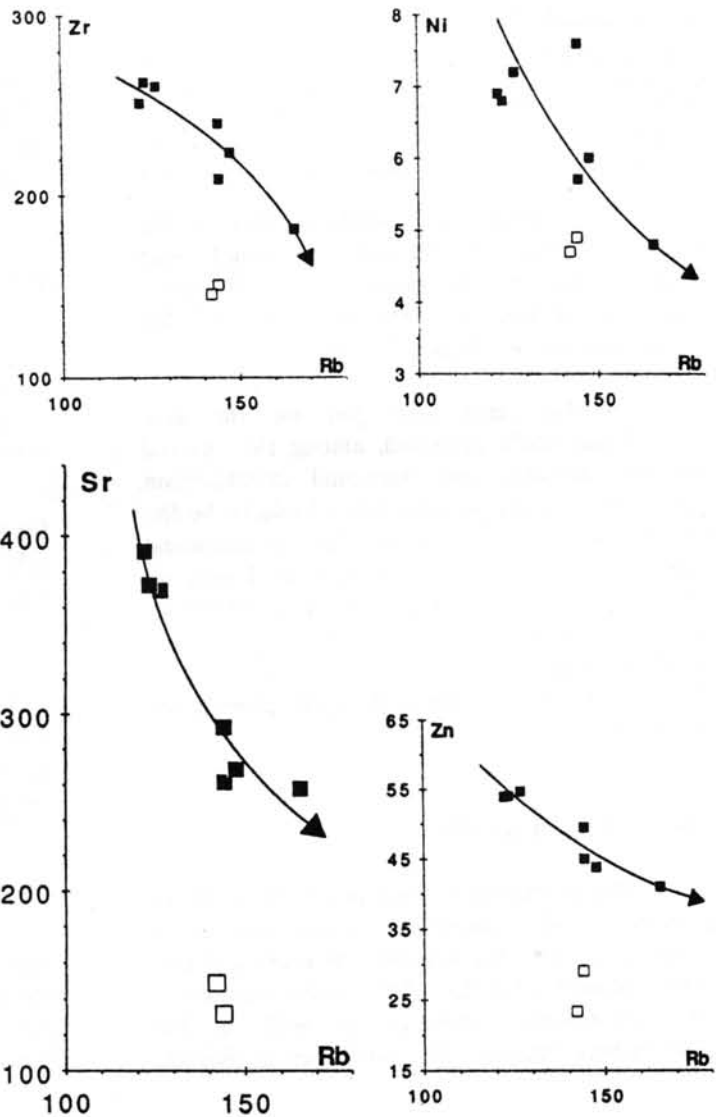


Figure III.18 - Compatible vs. incompatible element diagrams for Lagoa do Morro (■) and Serra dos Pombos (□) granitoids (after Marinho, 1991).

### The Rio Jacaré Sill

The Al-F-M diagram (Fig. III.23) of Besson & Fonteilles (1974) shows that notwithstanding a certain scattering due to cumulative phenomena, the data points of the Rio Jacaré sill, define a trend with an evolution close to that of the Skaergaard rocks (Wager, 1967) departing from the evolutions of the reference volcanic series used. The diagram emphasizes the strongly cumulative character of sample 228

The REE patterns for the lower and upper zones of the sill are shown in Fig. III.24 and a summary of these element ratios is seen in the table below:

	$(La/Yb)_N$	$(La/Sm)_N$	$(Gd/Yb)_N$	$Eu/Eu^*$
Upper zone	3.8 to 5.2	2.2 to 3.0	1.4 to 1.5	0.96 to 1.13
Lower zone	2.7 to 3.7	1.7 to 2.5	1.2 to 1.6	0.52 to 1.67

Fig. III.24 shows that the REE patterns of the upper and lower zone of the Rio Jacaré sill have similar shapes. The upper zone spectra are more fractionated [ $(La/Yb)_N = 3.8$  to  $5.2$ ] than those of the lower zone [ $(La/Yb)_N = 2.7$  to  $3.7$ ].

The behaviour of europium is variable in the rocks of the Rio Jacaré sill. The lower zone presents complementary spectra relatively to this element, with small or large anomalies, both positive ( $Eu/Eu^* = 1.03$  to  $1.67$ ) and negative ( $Eu/Eu^* = 0.52$  to  $0.64$ ). In the upper zone predominate small anomalies ( $Eu/Eu^* = 0.96$  to  $1.13$ ).

The existence of a slight difference in the fractionation of the REE between the upper and lower zone of the Rio Jacaré sill deserves some thought. In fact, within a process of fractional crystallization (which looks to be the case for the sill, as will be seen further on), the ratio between two incompatible elements is always constant for the same magmatic series (Treuil & Varet, 1973). Consequently the shapes of the REE curves does not depend on the degree of accumulation, only

the concentration levels may change. Thus, one must regard the possibility of existence of two different series to explain the difference between

the evolution of the upper and lower zones of the Rio Jacaré sill. This hypothesis is supported by the behaviour of Y and Zr (Fig. III.25) where the presence of these two series is also evidenced.

The petrographic and chemical features show the development of plagioclase accumulation vs. ferromagnesian minerals accumulation phenomena ("cumulats éclatés" in the sense of Fonteilles, 1976). This fact is sufficient to emphasize the essential role of fractional crystallization in the magmatic process that gave origin to the Rio Jacaré sill. It must be pointed out that the evolution of the Y/Nb and Zr/Nb ratios and of the  $\epsilon Nd_T$  (Fig. IV.28; chapter IV) are developed according to compatible trends of crustal contamination.

### The Transamazonian Granites

All granites occurring along the Jacobina-Contendas orogenic domain are peraluminous.

In the Contendas-Mirante belt, the aluminous index A of Debon & Le Fort (1982) clearly increases with the decrease of the mafic (biotite + oxides equivalent) B parameter interpreted as the degree of differentiation (Fig. III.26).

The geochemical behaviour leads to a similar distribution as shown by the petrographic characteristics (chapter B.3.4), the most differentiated and less peraluminous Lagoa Grande granite, on one hand, and the most peraluminous and diversified Lagoinha granite, on the other hand, encompasses the compositions of all the other leucogranites.

The differentiation trends, either in the Lagoinha or in the Gameleira plutons, underline an aluminous enrichment. The Lagoa Grande distribution is strongly homogeneous with low values of non-feldspathic alumina.

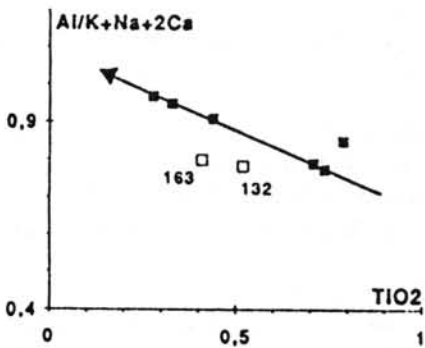


Figure III.19 -  $[(Al/(K+Na+2Ca))-(TiO_2)]$  diagram for the Pé de Serra granite: (■) = sub-alkaline rocks; (□) = alkaline rocks (after Marinho, 1991).

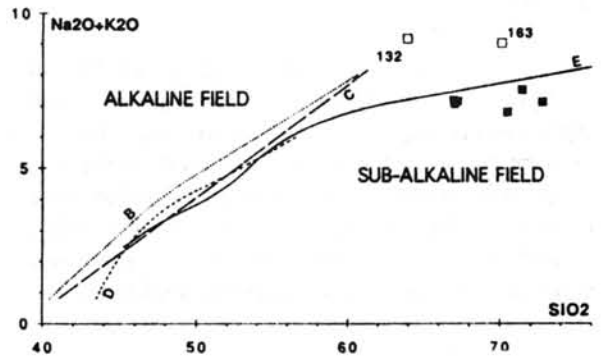


Figure III.20 -  $(Na_2O+K_2O)-(SiO_2)$  diagram for the Pé de Serra granite: (■) = sub-alkaline rocks; (□) = alkaline rocks. Sub-alkaline/alkaline domains limiting curves: (B) = Irvine & Baragar (1971); (Mac Donald & Katsura (1964); (D) = Hyndman (1972); (E) = Kuno (1968).

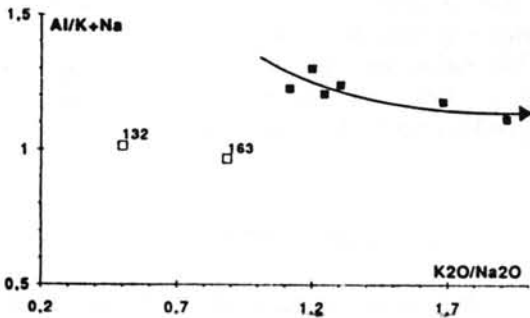


Figure III.21 -  $(Al/(Na+K))-(K_2O/Na_2O)$  diagram for the Pé de Serra granite: (■) = sub-alkaline rocks; (□) = alkaline rocks (after Marinho, 1991).

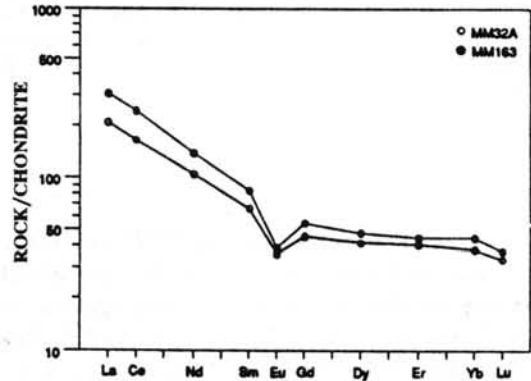


Figure III.22 - REE pattern of the Pé de Serra granite: (MM-32A) = sub-alkaline rock; (MM-163) alkaline rock (after Marinho, 1991).

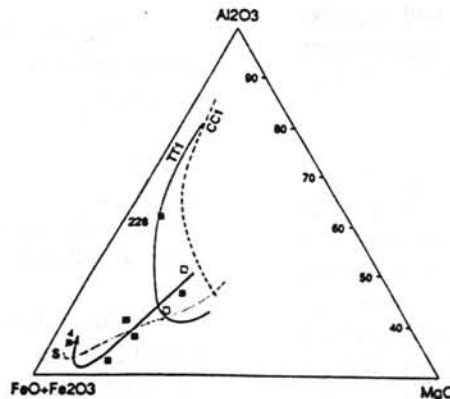


Figure III.23 - Besson & Fontelles (1974) AFM diagram for the Rio Jacaré mafic-ultramafic sill: (■) = upper zone; (□) = lower zone. (TT1) and (CC1) = tholeiitic and calc-alkaline series from Isu-Hakone volcano (Kuno, 1954); (S) = Skaergaard (Wager, 1967); (after Marinho, 1991).

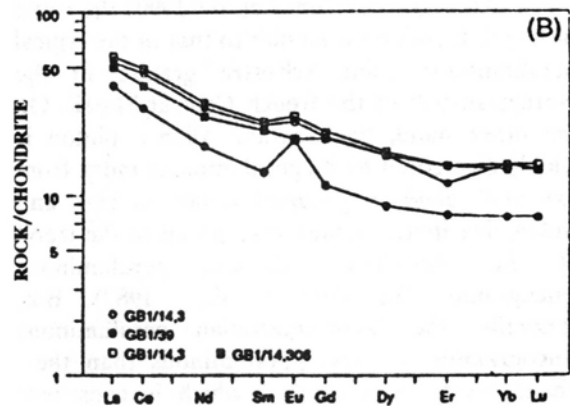
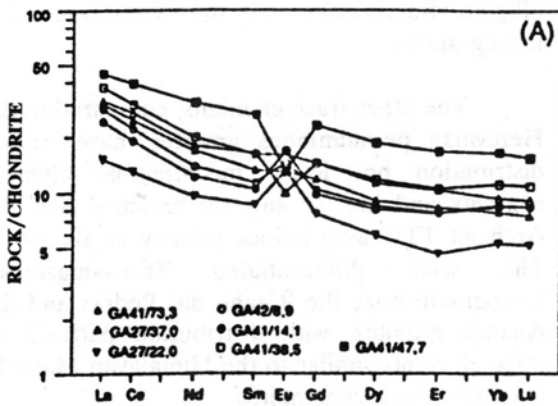


Figure III.24 - REE patterns of the Rio Jacaré mafic-ultramafic sill: (A) = lower zone; (B) = upper zone.

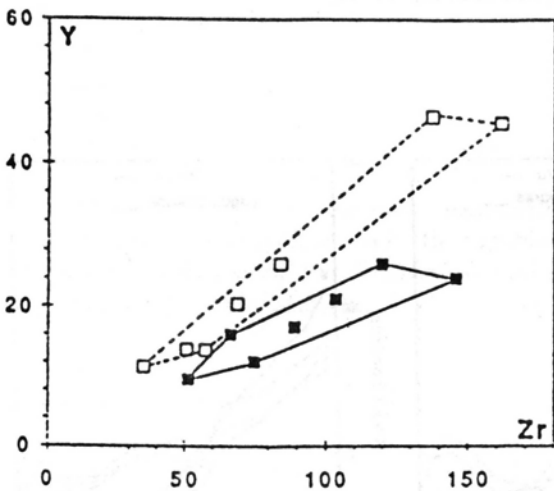


Figure III.25 - Y-Zr diagram for the Rio Jacaré mafic-ultramafic sill: (■) = upper zone; (□) lower zone.

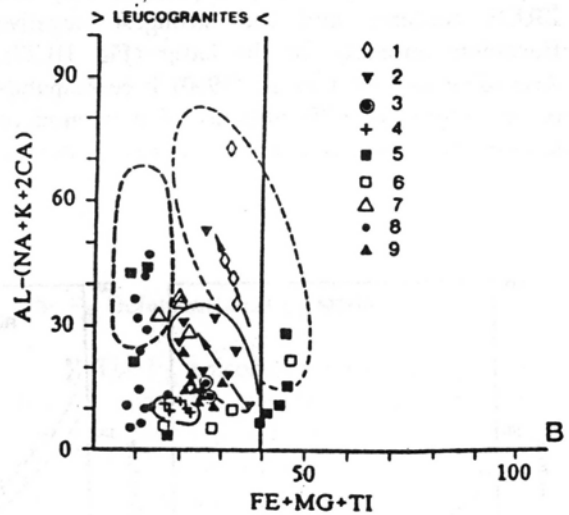


Figure III.26 - Debon & Le Fort (1982) diagrams showing the leucocratic and peraluminous character of the Transamazonian leucogranites and the Sete Voltas Archean granitoid. 1. Lagoinha; 2-3. Jacobina belt granites; 4. Lagoa Grande; 5-6. Sete Voltas; 7. Caetano/Aliaça; 8. Riacho das Pedras; 9. Gameleira. Light stippled line = composition field for the Hercynian Saint Sylvestre granite; heavy stippled line = composition field for the Himalayan Manaslu granite (from Le Fort et al., 1987). The arrows indicate the differentiation trends in a single pluton.

According to Cuney et al. (1990) the trend of Lagoinha pluton is similar to that of the typical peraluminous Saint Sylvestre granite in the Hercynian belt of the french Central Massif. On the other hand, the Caetano-Alliança pluton is widely diversified by its peraluminous index from low and relatively grouped values to high and widely distributed values superposed to the trend of the Himalayan Manaslu peraluminous leucogranite (Le Fort et al., 1987). But, generally, the Transamazonian peraluminous leucogranites are less peraluminous than their Phanerozoic equivalents, which is consistent with a low Al contents of the biotites of the former.

The REE patterns of the Lagoinha granite (Fig. III.27) are similar to the patterns of European and Himalayan Phanerozoic peraluminous granites (Vidal et al., 1982; Bernard-Griffiths et al., 1985) showing a weak fractionation of REE and negative Eu anomalies. The Caetano/Alliança and Gameleira granites display a "sea-eagle" shaped pattern, very low  $\Sigma$ REE contents and the strongest negative Europium anomaly for the latter (Fig. III.27). According to Cuney et al. (1990) it corresponds to the degree of differentiation like in modern leucogranites but, instead of monazite, with an

allanite fractionation in the Transamazonian leucogranites.

The other trace elements, compared to the Hercynian peraluminous granites, have similar distribution but lower incompatible element contents and are Sr and Ba enriched like the Archean TTG associations (Cuney et al., 1990). The most differentiated Transamazonian leucogranites are the Riacho das Pedras and the Alliança granites, with distribution patterns of trace elements similar to the Himalayan Manaslu peraluminous leucogranites.

Isotopic data support a crustal origin (Sabaté et al., 1990).  $Sr_i$  ratio of the granites (0.707 for Lagoinha, Lagoa Grande and Gameleira) are higher than the mantle ratios at the intrusion time (1974-1929 Ma), indicating a significant crustal residence time for the sources. The very high  $Sr_i$  value for the Riacho das Pedras (0.748) reflects either a fast increase during the magmatic stage (Vidal et al. 1979) of a Rb-rich highly evolved magma, as shown also by the major and trace element behaviour (Cuney et al., 1990), or an exchange with the country rocks, by hydrothermal activity through convective cell (Bonin et al., 1987).

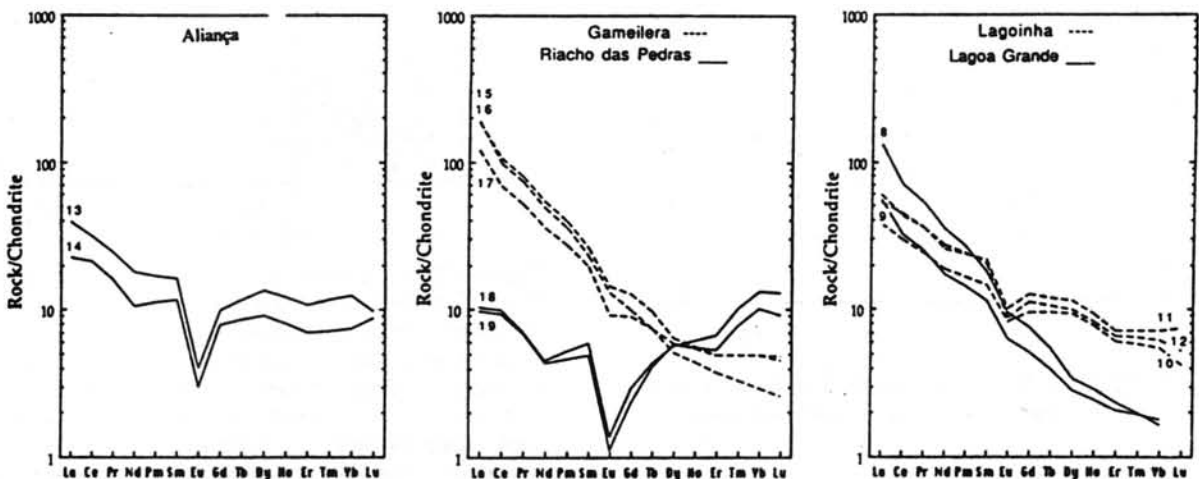


Figure III.27 - REE patterns of the Transamazonian leucogranites. (8-9) = Lagoa Grande; (10, 11, 12) = Lagoinha; (13-14) = Alliança; (15, 16, 17) = Gameleira; (18-19) = Riacho das Pedras (after Cuney et al., 1990).

The  $\epsilon_{Nd}$  values (-5.2 to -8.8) calculated on Sm-Nd results (Sabaté et al., 1990) are clearly negative and confirm the crustal origin of all these granites. It allows to establish, for each of them, a model age for the first extraction from a depleted mantle source. The ages range between ca. 2421 and 3265 Ma (Fig. IV.21, chapter IV).

As an attempt to constrain the sources of the Transamazonian peraluminous granites, the Nd isotopes are consistent with either the felsic and/or clastic rocks from the Contendas-Mirante sequence, or the Gavião block medium-grade terrains, but the related TTG are not good candidates because they are K depleted and their isotopic evolution does not cover the range of the granites (Fig. IV.21, chapter IV). The Jequié block granulitic terrain also may offer a good candidate for the source of the granite magmas, through the isotopic approach, but this hypothesis is ruled out by structural constraints (Sabaté and Gomes, 1984; Sabaté et al. 1990a, 1990b). In objection, the mineralogical and geochemical approach suggest that the Sete Voltas type Archean TTG suite may represent a possible source (Cuney et al., 1990).

Structural and kinematic features (Sabaté, 1991) as well as petrological, geochemical and isotopic constraints, support a geotectonic continent/continent collisional model, resulting in the Jacobina-Contendas orogenic alignment (FIG. III.3), built during the Transamazonian and concluded at 1.9 - 1.8 Ga (Sabaté et al., 1990) with the peraluminous leucogranitic magmatism. This model is compatible with the previous subducting evolution of the Contendas-Mirante sequence, proposed by Marinho (1991).

## STRUCTURAL FEATURES

The cartography of the belt (Marinho, 1978, 1979, 1980) synthesized by Marinho & Sabaté (1982) and completed in the northern portion by Silveira et al. (1984) indicates, as mentioned in the introduction, a huge N-S synform, branched into smaller belts in its northern and southern edges.

Internally, the synform presents a succession of imbricated second order antiforms complicated by thrusts and shear surfaces (Sabaté et al., 1980; Sabaté & Gomes, 1984).

## CONTINUOUS DEFORMATION IN THE CONTENDAS-MIRANTE SEQUENCE

In the field, the most evident and general feature is the interference of a two co-axial folding episodes (Fig. III.28), both related with coeval shear structures (Sabaté et al., 1980). Moreover, admitting these two regional folding phases, Jardim de Sá (1984) shows the existence of a previous folding phase, confined in the northeastern part of the belt, and of two more recent folding episodes weakly expressed (Fig. III.29).

The more recent structural compilation (Marinho, 1991) introduced a new nomenclature for the ductile continuous deformation episodes referred to the regional syn-schistose phase  $P_R$  which corresponds to the general structure of the belt responsible for the cartographic pattern and equivalent of  $P_2$  (from Sabaté et al., 1980) or  $F_3$  (from Jardim de Sá, 1984). The previous deformations correspond to the penetrative syn-schistose  $P_{R-1}$  phase, developed throughout the belt, and the locally expressed older one  $P_{R-2}$ .

### The $P_R$ Deformational Episode

The  $P_R$  episode corresponds to vertical or bended style non-cylindrical folds yielding the sub-meridian regional structure. It develops a penetrative crenulation schistosity  $S_R$  and lineations. A penetrative crenulation  $L_R$  and intersection  $L_{(S_0/S_R)}$  or  $L_{(S_{R-1}/S_R)}$  lineations occur widely.

The presence in the medium and upper sequences of sedimentation patterns such as graded bedding, turbidites and oblique stratifications alternately found in both normal or inverted positions, combined with the direct observation of intrafolial folds, isoclinal refolded folds giving interference patterns of the type -3 of

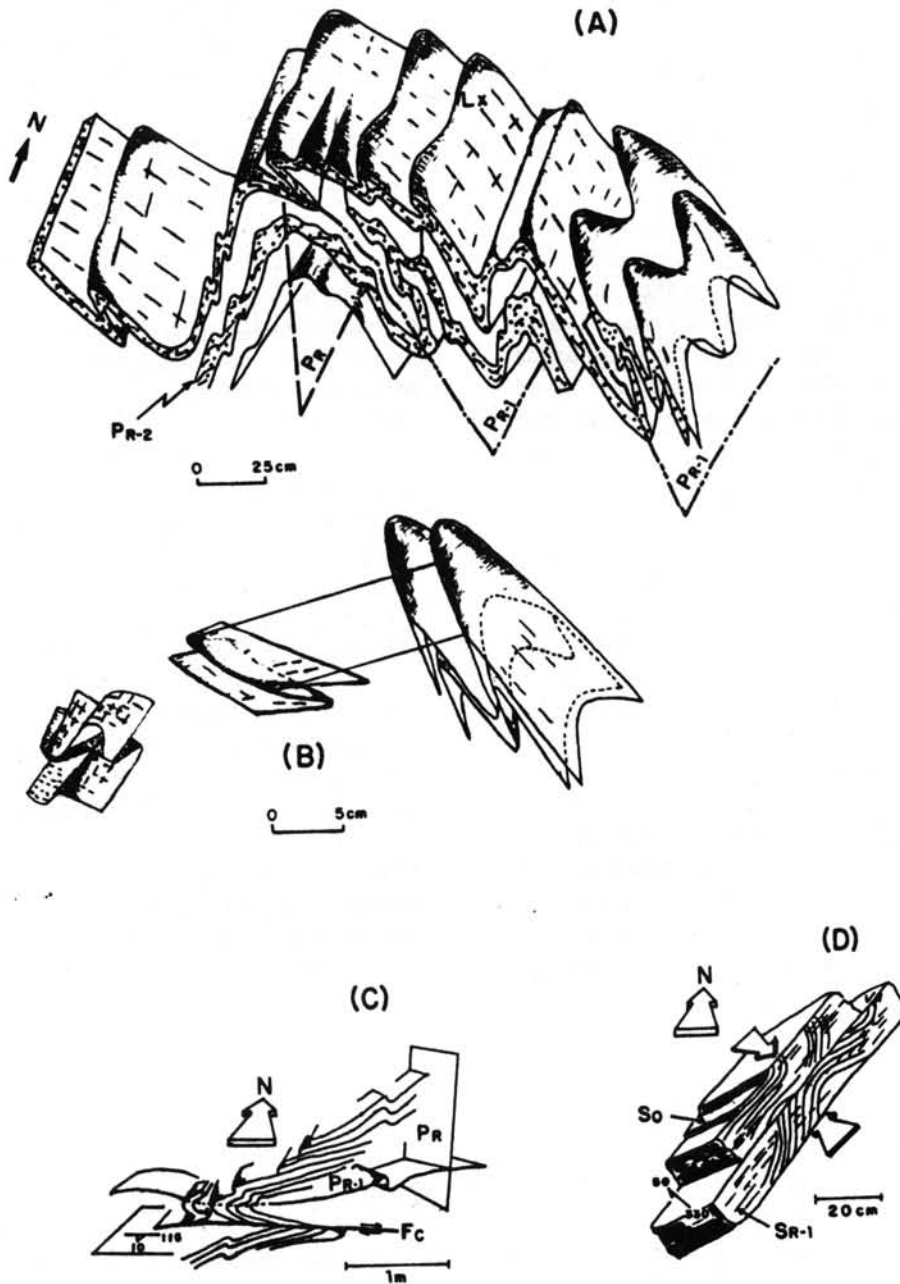


Figure III.28 - Main ductile deformations in the Contendas-Mirante sequence (after Marinho, 1991):  
 (A) Sketch diagram of type-3 fold interference pattern  $P_R/P_{R-1}$  and localized development of sheet folds (right part of the diagram), with  $L_x$  stretching lineation;  
 (B) Sketch diagram of type-2 fold interference pattern  $P_R/P_{R-1}$  developed on the curve axis of a  $P_{R-1}$  sheet fold (NNW rotated  $P_{R-1}$  axis);  
 (C) and (D) Shearing related with  $P_{R-1}$  folding (after Sabaté et al., 1980). (C) Shearing on the lower side of an isoclinal  $P_{R-1}$  horizontal fold. The westward displacement above the shear surface during  $P_{R-1}$  is reverted, on this west side of a  $P_R$  fold, during the reactivation by the  $P_R$  episode. (D) Shearing on foliation  $S_{R-1}$  planes. These  $S_{R-1}$  planes favour the development of shears during the  $P_R$  episode.

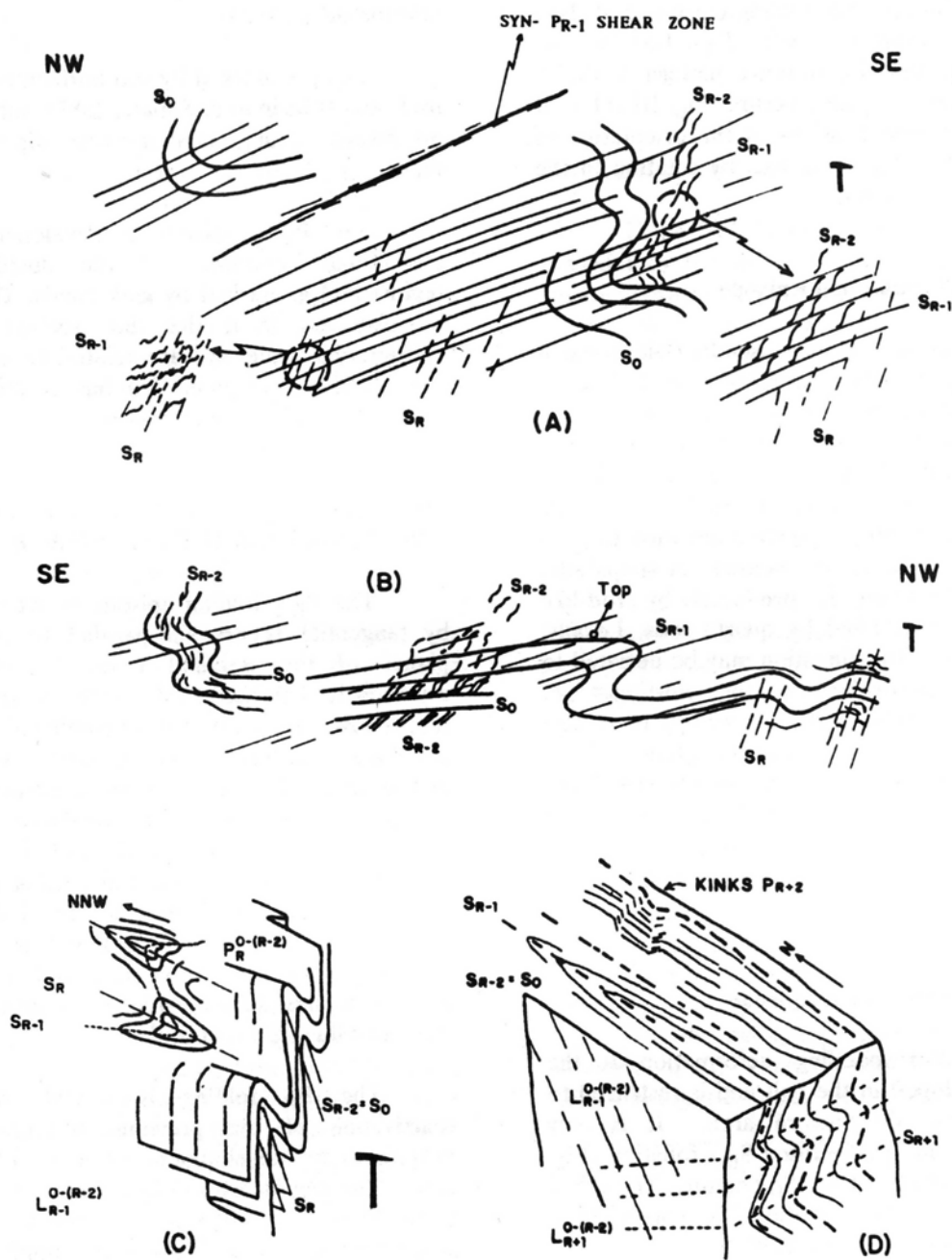


Figure III.29 - Sketch diagrams for the field relations of superposed deformational episodes in the Contendas-Mirante sequence (after Jardim de Sá, 1984):

(A) In the upper unit (Areião Formation): P<sub>R-1</sub> fold affecting the S<sub>0</sub> bedding. The related S<sub>R-1</sub> foliation crenulates the previous anastomosed S<sub>R-2</sub> foliation (detail on the left). This one cuts the S<sub>0</sub> bedding. The S<sub>R</sub> foliation, in its turn, crenulates the S<sub>R-1</sub> foliation (detail on the left);

(B) In the middle unit (Rio Gavião Formation): P<sub>R-1</sub> fold developing S<sub>R-1</sub> foliation which crenulates the anastomosed S<sub>R-2</sub> one;

(C) In the middle unit (Rio Gavião Formation): interference pattern P<sub>R</sub>/P<sub>R-1</sub> observed on S<sub>0</sub> + S<sub>R-2</sub> surface;

(D) In the middle unit (Rio Gavião Formation): late P<sub>R+1</sub> and P<sub>R+2</sub> deformation episodes observed on metapelites.

Ramsay (1967) (Fig. III.28A), evidence the existence of a previous folding episode and show its coaxial character with  $P_R$ . Locally, the "boomerang" type interference pattern of the 2-type of Ramsay (op.cit.) occurs (Fig. III.28B). It is related to modifications of the orientation of some previous  $P_{R-1}$  fold axis by rotation in the  $S_{R-1}$  plane (see below).

### The $P_{R-1}$ Deformational Episode

This episode is expressed by tight isoclinal folds, with variable amplitude and relative constant NNW axis. It is responsible for a metamorphic foliation or locally banding  $S_{R-1}$  which generally transpose the  $S_0$  stratification, except in the hinges of  $P_{R-1}$  folds. To this folding correspond a NNW intersection lineation  $L_{R-1}$  on  $S_0$  and  $S_{R-2}$  surfaces (see below). A subparallel stretching lineation is produced by rod-like fabrics and underlined by quartz rods. Locally, the direction of this lineation may be deviated to WNW, in particular to the northeast of Contendas do Sincorá city. According to Jardim de Sá (1984) it results from the rotation of the fold axis in the  $S_{R-1}$  plane, parallel to the X-axis of the finite strain, leading to the development of sheath folds. As this type of fold is only confined to this part of the belt, this author proposed this axis rotation mechanism.

### The $P_{R-2}$ Deformational Episode

The corresponding deformation is the earliest developed in the belt and is restricted to the Contendas do Sincorá area. It is only expressed by an anastomosed  $S_{R-2}$  foliation (Fig. III.28 A, B) which cut the  $S_0$  bedding. The effect of  $P_{R-1}$  on this  $S_{R-2}$  foliation is marked by a crenulation (Jardim de Sá, 1984).

### The Late $P_{R+1}$ And $P_{R+2}$ Deformational Episodes

After the regional ( $P_{R-1} + P_R$ ) structuration, two later fold episodes (Fig. III.29

D), at least, were superimposed on the belt (Jardim de Sá, 1984).

$P_{R+1}$  is marked by sub-horizontal chevron fold axis (Marinho & Sabaté, 1982), with a weak northward plunge and a north dipping axial plane.

The  $P_{R+2}$  episode is developed in the transitional conditions of the ductile/brittle regime and is marked by kink bands. These can be observed from the thin section to the cartographic scale and are related to a NE-SW and NW-SE conjugated faulting. It indicates a moderate N-S late compression.

### SHEARING AND THRUSTING IN THE CONTENDAS-MIRANTE SEQUENCE

The  $P_{R-1}$  folding episode is accompanied by tangential shears sub-parallel to the axial planes of the isoclinal folds. It results in asymmetric "fish-hook" folds with discontinuities on the lower side, which give, combined with the kinematic criteria, a general westward displacement. The resulting shear surfaces have an important expression at regional scale through the submeridian lineaments which often mark the contacts between lithologic units (Sabaté et al., 1980). They are responsible for the imbricated slices which control the present cartographic distribution of the lithological and structural units. The slices of the Archean basement were separated during this episode.

The  $P_R$  folding is coeval with the reactivation of the previous surfaces which propitiate the development of new N-S shear zones. This regional  $P_R$  deformation corresponds to an E-W shortening which tends to set the structures upright and allow the uplift of the Archean basement slices.

To the end of the shortening, corresponds a late, generally sinistral, horizontal shearing responsible for numerous Riedel synthetic NNW-SSE faults and tension gashes originating numerous quartz or baryte veins.

**STRUCTURAL RELATIONS BETWEEN THE BELT AND THE NEIGHBOURING CRUSTAL SEGMENTS**

As discussed above, the contact of the belt with the terrains related to the Jequié block is sharp, limited by repeated vertical shear bands which represent the upright setting of the thrust surfaces of the Jequié block.

In the southern part of the belt, east from the Serra dos Meiras massif, the contact is marked by the same thrusting discontinuity, but here the east-dipping ranges between 30° to 45°. Small "rags" of the volcano-sedimentary sequence are pinched and form several prisms which underline the tectonic contact between the Archean slice of the Serra dos Meiras and the lithologies of the overthrust granitic block (Sabaté & Gomes, 1984).

In the western part of the belt, the geometric shape is analogous, with a sharp contact marked by shears and faults which get upright through the P<sub>R</sub> deformational episode. These tectonic discontinuities may represent the reworked P<sub>R-1</sub> thrust surfaces which thrusts the Contendas-Mirante sequence onto the Gavião block.

**METAMORPHIC FEATURES**

The study of the metamorphism of the Contendas-Mirante volcano-sedimentary sequence was developed by Marinho (1991). The basic sampling was carried out in four sections: three in the northern part of the belt and a fourth one in the southeastern part, around the Boa Vista/Mata Verde granitoid. To these data are added those obtained by Marinho et al. (1979, 1980). These samples were subjected to determinations of whole-rock chemistry and mineral chemistry in electron microprobe.

Although that study has not dealt with the systematic cartography of the different isogrades it has yielded indispensable data for the understanding of the evolution of the metamorphism and the identification of the

regional metamorphic zoning of the Contendas-Mirante volcano-sedimentary sequence. It also allowed an estimation of the PT conditions of some zones of this metamorphism.

**METAMORPHIC ZONEOGRAPHY**

The establishment of this zoneography was based into the investigation of the metapelite-metagraywacke association of the middle unit. This assemblage of ample cartographic distribution allowed the application of the "method of the metamorphic zones" that consists in the comparison of the mineralogic assemblages of rocks with similar chemical composition; in this case once fixed the composition, the changes in the paragenesis depend on the different physical conditions of equilibrium.

The set of data obtained shows that the Contendas-Mirante volcanosedimentary sequence was submitted to a prograde metamorphism in the west-east sense, from the base to the top of the pile. The following metamorphic zones were defined:

- . chlorite zone;
- . biotite zone;
- . cordierite zone;
- . andaluzite zone;
- . sillimanite-muscovite zone;
- . sillimanite-K-feldspar zone.

The distinct parageneses and the stability domains of the minerals within each zone are shown in Fig. III.30 and the following table:

Minerals	Metamorphic Zones					
	Ch	BI	Cd	And	Sil-Mu	Sil+Fk
Mu						
Pl						
Ch						
BI						
Cd						
And						
Sil						
Fk						
St						
Gt						

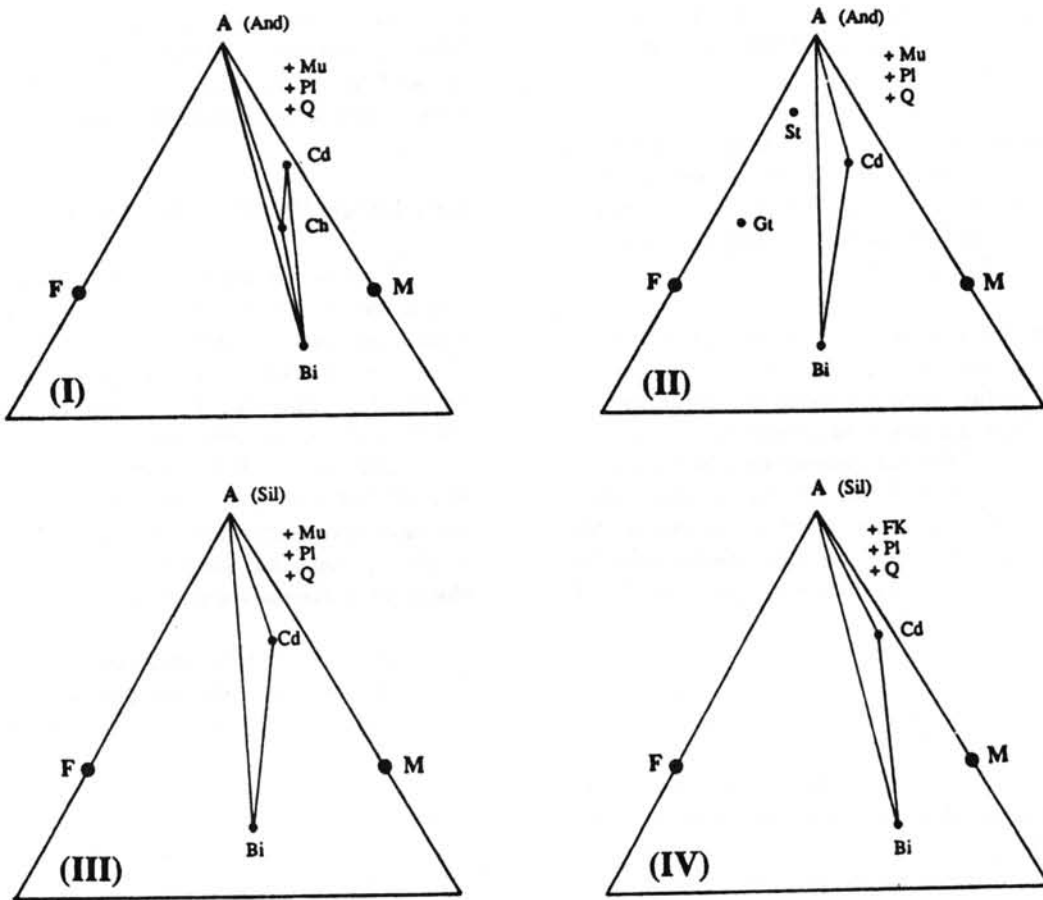


Figure III.30 - Thompson diagrams for the Contendas-Mirante middle unit metamorphic zones: (I) = cordierite zone; (II) = andalusite zone; (III) = sillimanite-muscovite zone; (IV) = sillimanite-potassic feldspar zone (after Marinho, 1991).

**ESTIMATES OF PHYSICO-CHEMICAL CONDITIONS OF METAMORPHISM**

The predominance of andalusite and cordierite mineral assemblages with rare garnet and estaurolite, allows the metamorphism of the Contendas-Mirante belt to be considered as of the low pressure type. The use of petrogenetic grids like those of Thompson (1976) and Yardley (1989), shows that the acting pressures were under 4 kb. More accurate indications of the P-T conditions of this metamorphism were obtained from the use of different geothermometers and geobarometers (Marinho, 1991).

**Geothermometry**

The geothermometric study developed was supported by the calibrations based in the garnet-biotite and garnet-cordierite pairs. Taking into account the scarcity of garnet in the area these thermometers could only be used for the andalusite zone. However, the existence of helictic garnets associated to the biotite and hornblende of the gabbros of the Rio Jacaré sill, that is in the sillimanite-muscovite zone, allowed the estimation of the temperature of this zone after the garnet-hornblende pair using the Graham and Powell (1984) calibration. The temperatures obtained in these thermometers in their several calibrations are shown in Tab. III-1.

Temperatures between 500 - 590°C for the andalusite zone and 580 - 630°C for the sillimanite-muscovite zone were obtained by the

several thermometers used. There are no available thermometers suited to the sillimanite-K feldspar zone but the formation of partial melts allows an estimation of the temperature using petrogenetic grids like those of Thompson (1976), Yardley (1989) and Myashiro (1973). For low pressures (close to 4 Kb) the melting starts at about 660°C.

**TABLE III-1 - Temperatures obtained with different thermometers and calibrations**

Zone	Thermometer	Calibrations	T (°C)
Andalusite	Biotite-garnet	(1),(2),(3), (4) and (5)	500-580
	Cordierite-garnet	(3) and (6)	500-560
Sillimanite	Biotite-garnet	(1),(2), (4) and (5)	580-610
	Garnet-hornblende	(6)	590-625

(1) Ferry and Spear (1978); (2) Thompson (1976); (3) Hodges and Spear (1982); (4) Perchuck and Aranovich (1984); (5) Holdaway and Lee (1977); (6) Graham and Powel (1984)

**Geobarometry**

The mineral associations which occur limit the application of geobarometry for the several metamorphic zones of the Contendas-Mirante belt. The presence of garnet in parageneses of the andalusite zone allowed the use of the following geobarometers:

- . garnet-plagioclase-biotite-muscovite;
- . garnet-cordierite;
- . garnet-plagioclase.

The estimated pressures after these geobarometers in their several calibrations are shown in Tab. III-2.

**TABLE III-2 - Pressures obtained with different barometers**

Geobarometer	Calibration	P (Kb)
Garnet-plagioclase-biotite-muscovite	(1)	2.90-3.18
Garnet-cordierite	(2)	2.90-3.15
Garnet-plagioclase	(3)	2.92-3.09

- (1) Ghent and Stout (1981)
- (2) Aranovitch and Podlesskii (1983)
- (3) Perchuck et al. (1985)

The comparison of the results obtained from different barometers point to a value between 2.9 and 3.2 Kb for the pressure of the andalusite zone of the regional metamorphism of the Contendas-Mirante belt.

**CONCLUSIONS ABOUT THE METAMORPHISM**

The Contendas-Mirante volcano-sedimentary sequence was affected by a W-E prograde regional metamorphism whose intensity is shown by the succession of six metamorphic zones.

The characteristic minerals of this metamorphism are cordierite and andalusite. The garnet (MnO 5-33 %) seldomly occur and staurolite is restricted to one sample.

The presence of andalusite and cordierite always in unoriented poikiloblastic nodules containing the foliations of the two main deformation episodes demonstrate their late development relatively to these deformations. However, it must be pointed out that inside the sillimanite-K feldspar zone, cordierite also appear in crystals surrounded by the foliation of the second main episode of deformation. The close association between the presence of this type of early cordierite and the Archean Boa Vista/Mata Verde domes seems to indicate the role of conductivity of these bodies, that allowed an easier ascent of the thermal front along the time, following a mechanism similar to the "basement effect" of Fonteilles & Guitard (1968).

The cordierite and/or andalusite

paragenesis are indicative of low pressure metamorphism. The use of the petrogenetic grids and the application of the different geothermometers and geobarometers gave more accurate indexes about the conditions of these metamorphism (Marinho, 1991):

METAMORPHIC ZONE	T (°C)	P (Kb)
Andalusite	500-580	2.9-3.2
Sillimanite-Muscovite	590-630	?
Sillimanite-K feldspar	≈ 660	?

This range of temperatures for the sillimanite zone is of the same order as those obtained by the garnet-biotite re-equilibrium in the granulitic rocks of Maracás region (Marinho, 1991). This re-equilibrium which appears to be coeval with other retrograde phenomena (destabilization of mesoperthites and transformation of red brown-greenish amphiboles into bluish-green amphiboles) of the granulitic rocks of the western border of the granulitic belt should be related to this prograde metamorphism of the Contendas-Mirante volcano-sedimentary sequence.